JACS
JOURNAL OF THE AMERICAN CHEMICAL SOCIETY

Article

pubs.acs.org/JACS

Alkynyl Phosphonate DNA: A Versatile "Click"able Backbone for DNA-Based Biological Applications

Heera Krishna and Marvin H. Caruthers*

Department of Chemistry and Biochemistry, University of Colorado at Boulder, Boulder, Colorado 80309, United States

Supporting Information

ABSTRACT: Major hurdles associated with DNA-based biological applications include, among others, targeted cell delivery, undesirable nonspecific effects, toxicity associated with various analogues or the reagents used to deliver oligonucleotides to cells, and stability toward intracellular enzymes. Although a plethora of diverse analogues have been investigated, a versatile methodology that can systematically address these challenges has not been developed. In this contribution, we present a new, Clickable, and versatile chemistry that can be used to rapidly introduce diverse functionality for studying these various problems. As a demonstration of the approach, we synthesized the core analogue, which is useful for introducing additional functionality, the triazolylphosphonate, and present preliminary data on its biological properties. We have developed a new phosphoramidite synthon—the alkynyl phosphinoamidite, which is compatible with conventional solid-phase oligonucleotide synthesis. Postsynthesis, the alkynylphosphonate can be functionalized via "Click" chemistry to generate the 1,2,3-triazolyl or substituted 1,2,3-triazolyl phosphonate-2′-deoxyribonucleotide internucleotide linkage. This manuscript describes the automated, solid-phase synthesis of mixed backbone oligodeoxyribonucleotides (ODNs) having 1,2,3-triazolylphosphonate (TP) as well as phosphate or thiophosphate internucleotide linkages and also 2′-OMe ribonucleotides and locked nucleic acids (LNAs) at selected sites. Nuclease stability assays demonstrate that the TP linkage is highly resistant toward 5′- and 3′-exonucleases, whereas melting studies indicate a slight destabilization when a TP-modified ODN is hybridized to its complementary RNA. A fluorescently labeled 16-mer ODN modified with two TP linkages shows efficient cellular uptake during passive transfection. Of particular interest, the subcellular distribution of TP-modified ODNs is highly dependent on cell type; a significant nuclear uptake is observed in HeLa cells, whereas diffuse cytoplasmic fluorescence is found in the WM-239A cell line. Cytoplasmic distribution is also present in human neuroblastoma cells (SK-N-F1), but Jurkat cells show both diffuse and punctate cytoplasmic uptake. Our results demonstrate that triazolylphosphonate ODNs are versatile additions to the oligonucleotide chemist's toolbox relative to designing new biological research reagents.

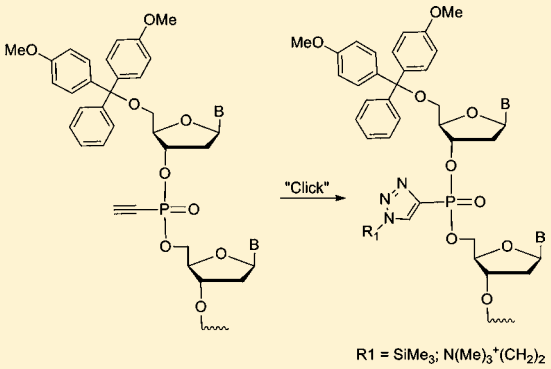

INTRODUCTION

Chemically modified, synthetic oligodeoxyribonucleotides (ODNs) 15−25 2′-deoxyribonucleotides in length act in a sequence-specific manner to modulate gene expression and thus have gained popularity in diverse areas of genomic research. These include, among others, their use as aptamers,[1] ribozymes,[2] enhancer DNA decoys,[3] CpG immunostimulatory oligomers,[4] diagnostic DNA chips,[5] and DNA-based functional nanomaterials.[6] ODNs having potential therapeutic drug applications are also being tested as antisense reagents,[1] triple helix-forming oligodeoxyribonucleotides (TFOs),[2] siRNAs,[3] and as antagomirs to microRNAs.[4,5] In order to be effective for various applications, these ODNs contain many modifications such as 2′-fluoro[7] to enhance nuclease resistance, a 2′-4′ methylene bridge[8] (LNAs) which enhances duplex melting temperatures, and cholesterol or other bioactive molecules[9] for increasing cellular uptake. However, given the repetitive nature of the reagents used during solid-phase synthesis and the considerable chemical functionality on these ODNs, the synthesis of highly modified ODNs is often cumbersome (synthons having difficult to prepare modifications are needed), involves numerous additional protection/deprotection steps, and occasionally suffers from low coupling efficiency which leads to poor overall yields. Postsynthetic modifications in solution phase are possible, especially when a biologically relevant analogue is unable to survive the harsh conditions employed during synthesis. Nevertheless, such postsynthetic functionalization needs to be highly efficient, specific, and result in the quantitative conversion of the ODN to the final, fully modified product.

The copper(I) catalyzed azide−alkyne [3 + 2] cycloaddition (CuAAC), developed by Meldal et al.[10] and Sharpless et al.[11] has emerged as the method of choice for postsynthetic modification of numerous biologically relevant molecules.[12] This is because the reaction is highly efficient, regioselective,

Received: March 19, 2012
Published: May 21, 2012

   dx.doi.org/10.1021/ja3026714 | J. Am. Chem. Soc. 2012, 134, 11618−11631

has a high pH tolerance range, retains facile synthetic accessibility of starting materials, and the alkynes and azides are inert to most biological and organic reaction conditions.[13] The reaction can be performed in water under ambient conditions[14] and generates a 1,4-disubstituted 1,2,3-triazolyl linkage that functions as a chemical linker for conjugating two desirable chemical or biological entities.

Apart from being a stable, biocompatible moiety, 1,2,3-triazoles have many appealing features. Due to high dipole moments, they are capable of hydrogen-bonding interactions through their N-atoms as well as dipole−dipole and π-stacking interactions with neighboring entities.[15] The aromatic character of the 1,2,3-triazole ring imparts chemical inertness to the linkage as well as stability toward reduction, oxidation and acid or base-catalyzed hydrolysis. These interesting electronic properties have led to their use as π-conjugated linkers in intramolecular electron transfer processes.[16] Owing to their ability to bind both cations and anions, they have been explored as chemical sensors,[17] and the presence of several donor sites for metal coordination (N3, N2, C5) has led to the development of the 'Click-to-chelate' approach wherein transition metal chelates are installed onto biomolecules in a single step.[18] It is noteworthy that 1,4-substituted 1,2,3-triazoles have been extensively employed as peptidomimetics owing to their structural and electronic similarity to a linear *trans*-peptide linkage.[19] They have also been explored as bioisosteres for internucleotide phosphate linkages.[20−23] Although 1,2,3-triazoles do not occur naturally, they are known to be biologically active, and their potency as pharmacophores has been reviewed.[24]

Despite the many desirable attributes of 1,2,3-triazoles, synthetic ODNs incorporating these heterocycles as backbone modifications have not been reported. However a literature search reveals that "Click" chemistry has been successfully applied to ligation, cyclization, bioconjugation, fluorophore labeling of DNA[25] and RNA,[26] synthesis of modified nucleosides,[27] PNA−DNA chimeras,[28] DNA−carbohydrate dendrimers,[13] site-specific labeling of siRNA for targeted delivery[29] and coupling ODNs to monolayers.[30] These postsynthetic functionalizations of DNA by CuAAC involves the use of alkyne-modified dU phosphoramidites,[31] phosphoramidites derived from alkyne-labeled 7-deazapurines and pyrimidines,[32] and 2′-*O*-alkynyl-modified sugars.[33] Click chemistry at the phosphorus center has not been explored except for functionalization at the 5′-position of a DNA strand. For example, an oligodeoxynucleotide containing a single 5′-phosphate triester appended to a long spacer arm with a terminal alkyne has been used for template-mediated chemical ligation with a 3′-azide-modified oligodeoxynucleotide.[25] Additionally recent reports describe the synthesis of phosphoramidites containing one, two, or three alkyne functions appended to a phosphate triester via a side-chain, and introduced at the 5′- end of oligodeoxynucleotides.[34,35] The only attempt at multiple functionalization of the phosphate backbone with triazolyl linkages using the phosphate triester methodology has been unsuccessful owing to the instability of the triazolyl-containing triester side chain toward the basic cleavage conditions required for chemical synthesis.[36]

We hypothesized that a more attractive synthetic target would be a P−C linked triazolyl phosphonate because it would be resistant to degradation during both synthesis and biological studies. Given the metabolic inertness of triazoles,[37,38] we also hypothesized that such an ODN might have excellent stability toward nucleases and possess favorable hydrogen-bonding and solubility properties. An added advantage would be the inherent modularity of the Click approach as it permits further modifications of the chemical and/or biological properties of the ODN by appending cellular targeting ligands or other desirable functionalities to 1,2,3-triazoles.

In order to test our hypothesis, we developed a novel backbone modification—the 1,2,3-triazolylphosphonate internucleotide (TP) linkage wherein one of the nonbridging oxygen atoms of phosphate is replaced by a 1,2,3-triazole moiety linked to phosphorus via C4 of the triazole ring. TP linkages are generated as a two-step process. Initially the ethynylphosphonate internucleotide linkage is introduced at designated sites with conventional phosphoramidite chemistry and automated solid-phase synthesis. The next step is to use CuAAC to introduce the appropriate azide before deprotection and cleavage from the solid support.[39] By coupling these two steps, we have synthesized chimeric ODNs (16−23mers) that contain up to six TP modifications as well as other functionalities such as LNA nucleotides, 2′-OMe ribonucleotides, and thiophosphate. We have studied the thermal stability and nuclease resistance of these ODNs and explored their utility as efficient self-delivery agents. The results of these experiments and the unique subcellular localization patterns of TP ODNs in different cell lines have encouraged us to continue investigating their potential as antagomirs for targeting microRNA expression.

In this contribution, we describe the chemical synthesis of nucleoside 3′-*O*-alkynylphosphinoamidites, solid-phase synthesis protocols, hybridization experiments (T_m), nuclease susceptibilities, and preliminary in vivo studies on a series of mixed-sequence ODNs having 1,2,3-triazolylphosphonate internucleotide linkages.

RESULTS AND DISCUSSION

Copper-catalyzed azide−alkyne cycloadditions (CuAAC) have been successfully employed using nucleosides that are alkynylated at the 5′-, 2′-, or 3′-hydroxyls which generates the corresponding *O*-propargylated derivatives.[29] A major breakthrough from the Carell group has enabled high-density conversion of alkyne functions on ODNs containing up to six consecutive alkyne-modified nucleobases.[31] This was accomplished by introducing a long spacer arm between the nucleobase and the alkyne functionality, thus making it more accessible to Click reagents. Morvan et al. have synthesized phosphoramidite building blocks having phosphorus appended to the alkynyl function through a P−O linkage.[34,35] However, owing to the inherent lability of phosphotriesters toward basic deprotection and cleavage conditions, this type of linkage would be partially lost during synthesis.

Indeed, Tanabe et al. recently reported that aqueous methylamine (20 h, 40 °C), which is used to remove ODNs from a support, can effectively hydrolyze Click functionalized side chains tethered by a P−O linkage to give unmodified DNA.[36] To overcome this limitation, we developed an alkynyl functionalized phosphinoamidite that was joined to phosphorus by a P−C as opposed to a P−O linkage. Using this synthon, oligodeoxyribonucleotides having alkynylphosphonates at selected sites were first synthesized on a solid support. Triazolylphosphonate was then introduced using an appropriate azide via the CuAAC method. This approach has the advantage that excess Click reagents can be used for better product yields and then removed simply by washing the

dx.doi.org/10.1021/ja3026714 | J. Am. Chem. Soc. 2012, 134, 11618−11631

Scheme 1. Synthesis of 5′-*O*-Dimethoxytrityl-3′-*O*-ethynyl-2′-deoxyribonucleoside Phosphinoamidite and Generation of a Triazolylphosphonate Internucleotide Linkage[a]

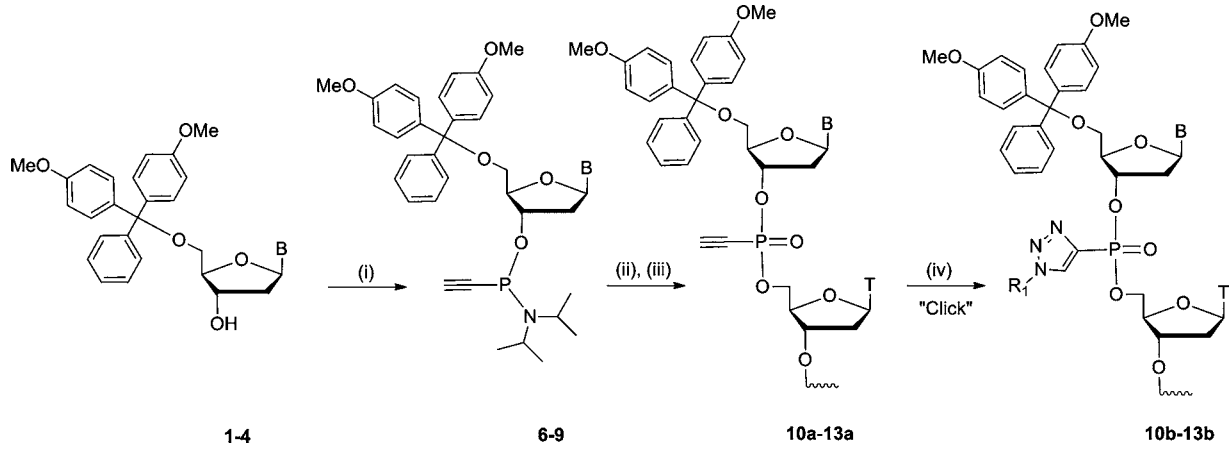

[a]Reaction conditions: (i) 1.1 equiv of $HC{\equiv}CP[N(i\text{-}C_3H_7)_2]_2$ (**5**), CH_2Cl_2, 1*H*-tetrazole, 60 min; (ii) 2′-deoxyribonucleoside linked to a solid support through the 3′ hydroxyl, 0.25 M 5-ethylthio-1*H*-tetrazole, CH_3CN, 600s; (iii) 0.02 M iodine in THF/water/pyridine; (iv) $R_1{-}N_3$ (6 equiv), where R_1 = $SiMe_3$ or $N(Me)_3{}^+CH_2CH_2$, $CuSO_4{\cdot}5H_2O$ (0.8 equiv), sodium ascorbate (6 equiv), tris(1-benzyl-1*H*-1,2,3-triazol-4-yl)methylamine (7 equiv) in H_2O/MeOH/THF (1.2 mL, 2:2:1 v/v/v).

support prior to deprotection of the bases and cleavage of the ODN from the solid phase.

Chemical Synthesis. Our initial objective was to prepare ethynylphosphinoamidite synthons of the four 2′- deoxyribonucleosides (**1**−**4**). This strategy would allow us to introduce the TP linkage at any selected site. The phosphitylating reagent, bis(*N*,*N*-diisopropylamino)ethynyl phosphine (**5**), was synthesized in high yield (90%) via a Grignard reaction from bis(*N*,*N*-diisopropylamino)chlorophosphine and ethynylmagnesium bromide.[40] This phosphine was allowed to react with the appropriate N-protected 5′-O-DMT-2′-deoxyribonucleoside (A, G, C) or 5′-O-DMT-2′-deoxythymidine to yield 5′-O-DMT-2′-deoxyribonucleoside-3′-O-ethynylphosphinoamidite (Scheme 1, Compounds **6**−**9**). These synthons were obtained in high purity after column chromatography with average yields ranging from 40 − 66%. Characterization by NMR and mass spectral analysis (see Experimental Section) confirmed the assigned structures.

Solid-Phase Synthesis. Chimeric ODNs having TP, phosphate, and thiophosphate internucleotide linkages as well as 2′-deoxyribonucleoside, 2′-OMe ribonucleoside, or LNA nucleosides were synthesized on solid supports using ethynylphosphinoamidites **6**−**9**, the commercially available 5′-O-DMT-2′-deoxyribonucleoside 3′-O-phosphoramidites, and the corresponding 3′-O-phosphoramidites of 2′-OMe ribonucleosides and LNAs. Table S1(Supporting Information [SI]) summarizes the synthesis cycle. Briefly, the coupling wait time was increased to 600 s for synthons **6**−**9**, whereas the reaction time for the remaining nucleoside phosphoramidites was according to the manufacturers' specifications. The activator was 5-ethylthio-1*H*-tetrazole (0.25 M in anhydrous acetonitrile). After each condensation step, the support was washed with acetonitrile for 40 s and failure sequences blocked using Unicap phosphoramidite (Glen Research). Standard oxidation with 0.02 M iodine in THF/water/pyridine generated phosphate or alkynylphosphonate. The phosphorothioate internucleotide linkage was prepared using Beaucage reagent[41] as the oxidant. These synthesis steps were repeated until the ODN of the desired sequence/length was prepared. Postsynthesis, the support was removed from the column and placed in a 1.5 mL screw-cap glass reaction vial. The CuAAC reaction was then carried out using the appropriate azide. A heterogeneous mixture of the solid-support bound ODN (1.0 μM) and a solution of H_2O/MeOH/THF (1.2 mL, 2:2:1 v/v/v) containing azide (6 equiv based upon the alkyne), $CuSO_4{\cdot}5H_2O$ (0.8 equiv), freshly prepared sodium ascorbate (6 equiv), and tris[(1-benzyl-1*H*-1,2,3-triazol-4-yl)methyl]-amine (TBTA,7 equiv) was allowed to react at room temperature for 7 h to obtain the triazolyl phosphonate ODN. The support was then washed successively with water (2 × 20 mL), methanol (2 × 10 mL), acetonitrile (2 × 10 mL) and dichloromethane (2 × 10 mL). After drying, a 1:1 solution (2 mL) of anhydrous ethylenediamine in toluene was added, the support stirred by vortexing, and cleavage of the ODN was allowed to proceed to completion over 2 h at room temperature. The cleavage mixture was discarded[42] and the solid-support evaporated to dryness in a SpeedVac. The crude ODN was washed from the support with 5% acetonitrile in water (1 mL) and purified by RP-HPLC using a linear gradient of 0 to 100% B over 40 min at a flow rate of 1.5 mL/min (buffer A: 50 mM TEAB, pH 8.5; buffer B: acetonitrile). The trityl-on fractions were combined, evaporated to dryness in a SpeedVac, and treated with an 80% acetic acid solution for 2 h in order to remove the trityl group. A second RP-HPLC was then carried out to enhance the purification. A similar HPLC profile was obtained for all ODNs, with the capped failure sequences eluting at ∼20 min, whereas the trityl-on product was observed at ∼35 min. Broad product peaks were anticipated due to the presence of multiple chiral phosphorus centers. The average yields (95% purity) for a 1.0 μM synthesis ranged from 120 to 200 OD. An ODN that required a fluorescein tag was synthesized as trityl-off and the last coupling was completed with a commercially available fluorescein phosphoramidite (Glen Research, VA). Aliquots of all ODNs were characterized by analytical HPLC. Figures S7−S11 in the SI show analytical RP-HPLC profiles for ODNs **1**, **3**, **5**, **10**, and **11** respectively. The mass data for selected ODNs having a combination of TP, phosphate, or thiophosphate internucleotide linkages and 2′-deoxyribonucleosides, 2′-OMe ribonucleosides, and LNA nucleosides are listed in Table 1. Even after two

dx.doi.org/10.1021/ja3026714 | J. Am. Chem. Soc. 2012, 134, 11618−11631

Table 1. ODN Sequences used for NMR, T_m studies, and Molecular Weight Analysis

		mol wt	
no	ODNs[†]	calc	obs
ODN 1	$A_a\ C_pC_aA_a\ T_aG_pA_a\ T_pG_pT_p\ G_pC_pT_p\ G_pC_pT$	5125.9	5190.0
ODN 2	$T_pG_pT_a\ A_pA_aA_p\ C_aC_pA_a\ T_pG_pA_a\ T_aG_pT_p\ G_pC_pT_p\ G_pC_pT$	6741.2	6805.6
ODN 3	$T_aG_pT_p\ A_pA_aA_p\ C_aC_pA_a\ T_pG_pA_a\ T_pG_pT_p\ G_pC_pT_p\ G_pC_pT_p\ A_aT$	7360.3	7423.1
ODN 4	$U_p^{Me}G_aU_p^{Me}\ A_p^{Me}A_aA_p^{Me}\ C_aC_p^{Me}A_a\ U_p^{Me}G_p^{Me}A_a\ U_p^{Me}G_p^{Me}U_p^{Me}\ G_p^{Me}C_p^{Me}U_p^{Me}\ G_p^{Me}C_p^{Me}U_p^{Me}\ A_p^{Me}U^{Me}$	7753.4	7817.2
ODN 5	$T_aG_p^{Me}U_p^{Me}\ A_p^{Me}A_aA_p^{Me}\ C_aC_p^{Me}A_a\ U_p^{Me}G_p^{Me}A_a\ U_p^{Me}G_p^{Me}U_p^{Me}\ G_p^{Me}C_p^{Me}U_p^{Me}\ G_p^{Me}C_p^{Me}U_p^{Me}\ A^{Me}$	7416.3	7480.5
ODN 6	$T_pG_p^{Me}U_p^{Me}\ A_p^{Me}A_pA_p^{Me}\ C_pC_p^{Me}A_p\ U_p^{Me}G_p^{Me}A_pU_p^{Me}G_p^{Me}U_p^{Me}\ G_p^{Me}C_p^{Me}U_p^{Me}\ G_p^{Me}C_p^{Me}U_p^{Me}\ A^{Me}$	7161.2	7163.5
ODN 7	$A_p^{Me}\ C_aC_p^{Me}A_a\ U_p^{Me}G_p^{Me}A_a\ U_p^{Me}G_s^{Me}U_p^{Me}\ G_s^{Me}C_p^{Me}U_p^{Me}\ G_s^{Me}C_p^{Me}U_s^{Me}\ A_aT$	5762.9	5827.4
ODN 8	$T_aG_p^{Me}U_p^{Me}\ A_p^{Me}A_aA_p^{Me}\ C_aC_p^{Me}A_a\ U_p^{Me}G_p^{Me}A_a\ U_p^{Me}G_s^{Me}U_p^{Me}\ G_s^{Me}C_p^{Me}U_p^{Me}\ G_s^{Me}C_p^{Me}U_s^{Me}\ A_aT$	7751.3	7813.4
ODN 9	$T_pG_p^{Me}U_p^{Me}\ A_p^{Me}A_pA_p^{Me}\ C_pC_p^{Me}A_pU_p^{Me}G_p^{Me}A_p\ U_p^{Me}G_s^{Me}U_p^{Me}\ G_s^{Me}C_p^{Me}U_p^{Me}\ G_s^{Me}C_p^{Me}U_s^{Me}\ A_pT$	7510.2	7511.1
ODN 10	$A_aC_pC_a\ A_pT_p^{L}G_p\ A_aT_p^{L}G_p\ T_pG_pC_p\ T_pG_pC_p\ T_pA_aT$	5130.9	5195.4
ODN 11	$T_p^{L}G_p\ T_pA_aA_p\ A_aC_pC_a\ A_pT_p^{L}G_p\ A_aT_pG_p\ T_pG_pC_p\ T_pG_pC_p\ T_pA_aT$	7363.3	7427.5
ODN 12	$T_p^{L}G_p\ T_pA_pA_p\ A_pC_pC_pA_pT_p^{L}G_p\ A_pT_pG_p\ T_pG_pC_p\ T_pG_pC_p\ T_pA_pT$	7108.2	7109.3
ODN 13	$T_p^{L}G_p\ T_pA_aA_p\ A_aC_pC_a\ A_pT_p^{L}G_p\ A_aT_pG_p\ T_p^{L}G_pC_p\ T_p^{L}G_pC_p\ T_p^{L}A_aT$	7448.3	7513.3
ODN 14	$T_p^{L}G_p\ T_pA_pA_p\ A_pC_pC_pA_pT_p^{L}G_p\ A_pT_pG_p\ T_p^{L}G_pC_p\ T_p^{L}G_pC_p\ T_p^{L}A_pT$	7193.2	7194.4

[†]Subscripts: "p", phosphate; "s", thiophosphate; "a", 1,2,3-triazolylphosphonate. Superscripts: "Me" represents a 2′-OMe ribonucleoside; "L" denotes a LNA nucleoside. All ODNs have 2′-deoxyribonucleosides except where designated as 2′-OMe ribonucleoside or LNA.

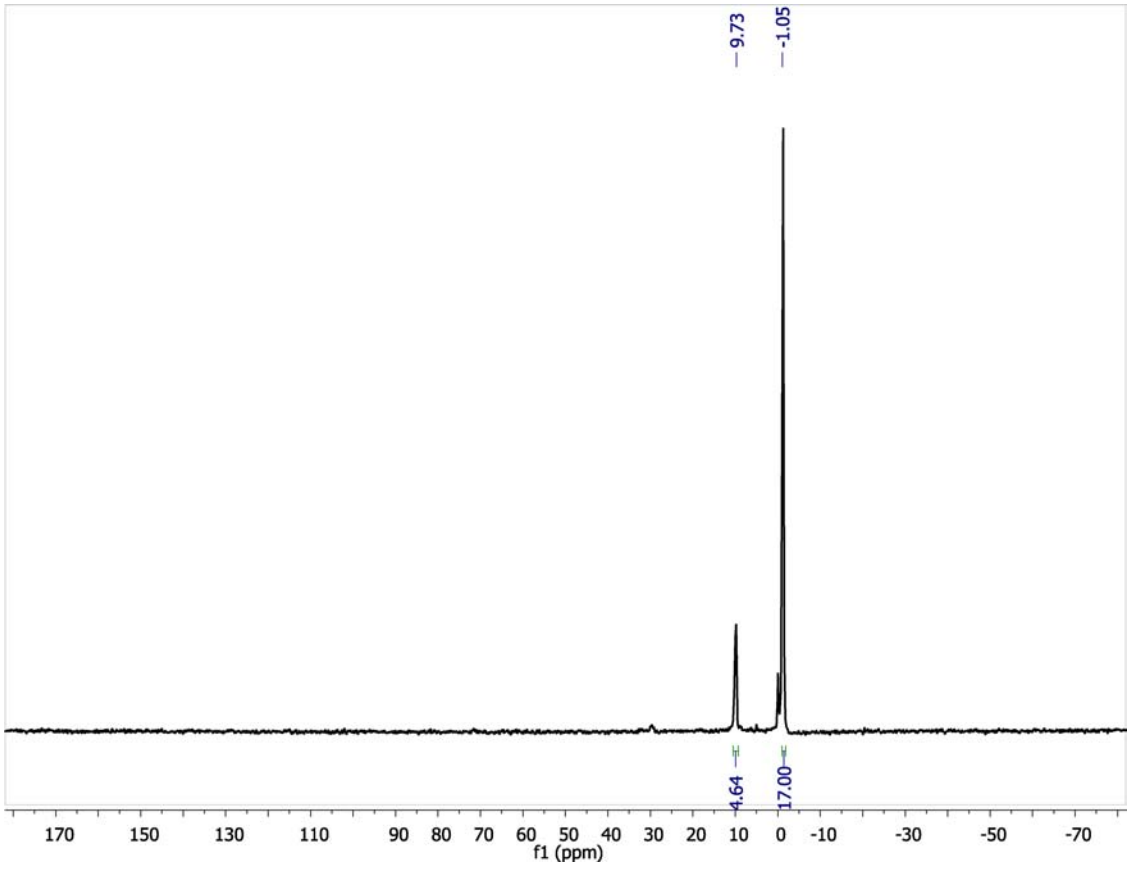

Figure 1. ^{31}P NMR spectrum of ODN **4** (300 MHz, D_2O, 13,064 scans) ($U_p^{Me}G_aU_p^{Me}A_p^{Me}A_aA_p^{Me}C_aC_p^{Me}A_aU_p^{Me}G_p^{Me}A_aU_p^{Me}G_p^{Me}U_p^{Me}G_p^{Me}C_p^{Me}U_p^{Me}A_p^{Me}U^{Me}$) (See Table 1 for an explanation of these abbreviations.).

RP-HPLC purification and desalting (illustra NAP-10 columns, GE Healthcare), chelated copper ions were detected during the mass spectral analysis. Washing the solid-support with an EDTA solution prior to cleavage did not remove the copper adducts. The observed peaks were broad, the m/z values were higher than the expected mass and corresponded to one or more copper adducts (see Table 1). This phenomenon has been reported earlier[29,43] and copper toxicity remains one of the major potential problems with the copper-catalyzed "Click" chemistry approach. This is because copper ions exhibit a high affinity for thiol groups and may therefore severely hamper many metabolic functions in the cell. Copper also catalyzes the generation of highly reactive triplet oxygen species that can degrade oligonucleotides[44] and induce cytotoxicity in biological systems.[45,46] The interactions of copper with nucleotides and nucleic acids have been studied extensively in the past.[47] It is well-known that there are two main sites of interaction of copper with DNA, namely the phosphate backbone and the

dx.doi.org/10.1021/ja3026714 | J. Am. Chem. Soc. 2012, 134, 11618−11631

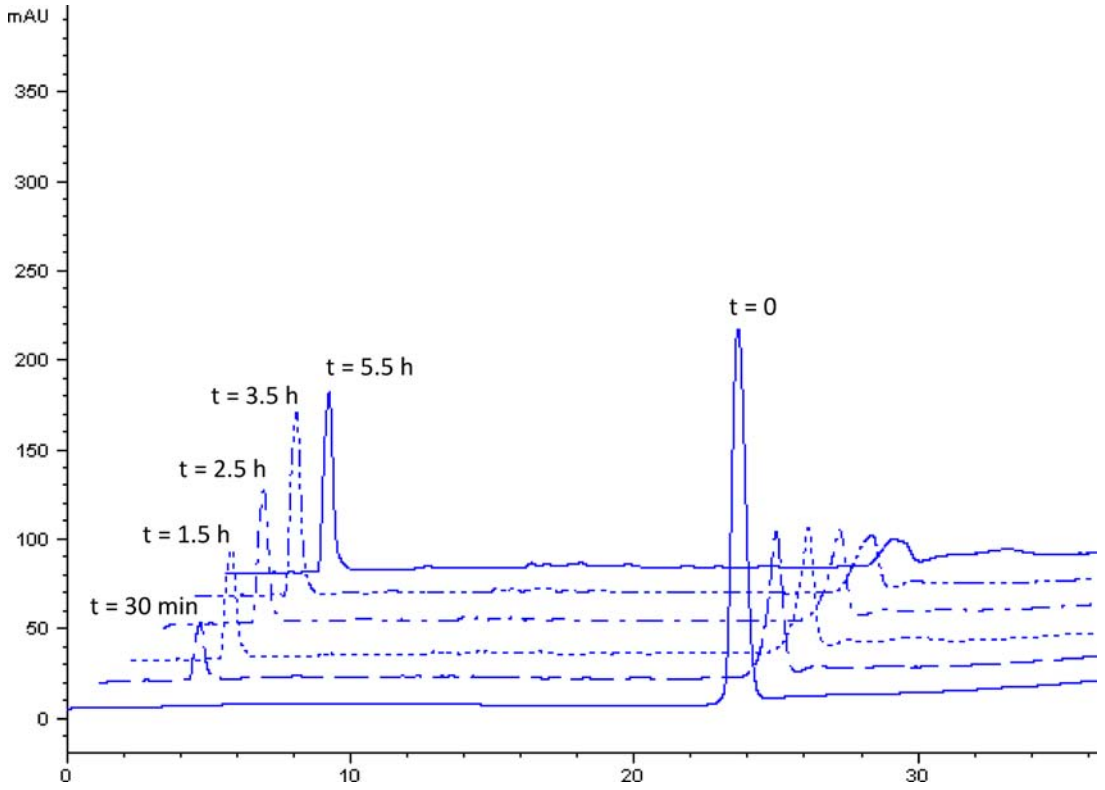

Figure 2. Time-dependent enzymatic hydrolysis of ODN **T4** in the presence of SVPDE.

electron-donor groups on the nucleoside bases. The ratios of nucleoside base/phosphate binding affinities for the early transition metals follow the order Mg(II) < Co(II), Ni (II) < Mn (II) < Zn (II) < Cd(II) < Cu(II). Thus, copper ions are known to exhibit the greatest affinity for nucleoside bases.[48] As indicated by several studies,[49,50] Cu^{2+} may attach initially to phosphate and later become bound to the bases since its binding affinity (K_a) to the nucleosides is greater by an order of 10^2 M^{-1}.[51] Hence it is unclear whether the copper in the ODNs prepared here is bound to phosphate or the nucleoside bases.

The ^{31}P NMR analyses of ODNs display a signal at 9.7 ppm (TP), and a sharp peak at −1.05 ppm (phosphate) (Figure 1). ^{31}P NMR chemical shifts in the range 8.0−10.3 ppm have been reported for bis(2-chloroethyl)-1H-1,2,3-triazolylphosphonates.[52] Similar chemical shifts have also been reported for a series of stable triazolylalanine phosphonate analogues.[53]

All ODNs used for biological studies were purified by PAGE and desalted using illustra NAP-25 columns (GE Healthcare). Polyacrylamide-gel electrophoresis of ODNs having variable numbers of triazolyl phosphonate linkages was carried out using an unmodified oligodeoxyribonucleotide as a marker in order to determine the effect of this modification on electrophoretic mobility. As anticipated, mobility decreased with an increase in TP modifications due to charge neutralization of the phosphate backbone. Using a series of polythymidylate 16-mer ODNs (**T1**, **T2**, and **T3**), **T3** having six TP modifications had reduced mobility when compared to **T2** with four modifications. Similarly **T1** with only two modifications had increased mobility relative to **T2** (Supporting Information, Table S2). Neutralization of the DNA phosphate backbone is desirable for many applications. Charge neutralized backbones have been shown to improve DNA flexibility which enhances protein-induced bending.[54] It can also augment DNA-binding motifs in DNA−protein recognition processes,[55] improve hybridization to a complementary strand,[56] aid transport of ODNs across biomembranes[57] and prevent cleavage by RNase H.[58,59] An added advantage of the TP linkage is retention of aqueous solubility despite the backbone charge neutralization since the triazole ring can engage in hydrogen-bonding interactions with neighboring entities. The P−Me or other alkyl or arylphosphonate hydrophobic backbone modifications do not possess these characteristics and exhibit significant solubility concerns.[60]

Enzymatic Studies. Since unmodified DNA is rapidly degraded by cellular nucleases, one of the key requirements for synthetic DNA analogues employed in biological research is that they are nuclease resistant in subcellular environments. Among chemically modified ODNs, the nuclease stability of the nonionic methylphosphonate P−C bond as a substitute for P−O has been thoroughly investigated.[61,62] Because of these studies, triazolylphosphonates were appealing since the P−C bond was expected to be both nuclease resistant and have enhanced aqueous solubility due to improved hydrogen bonding.[53]

To evaluate the relative exonuclease susceptibility of triazolylphosphonate modified ODNs, we synthesized two 23-mer polythymidylate ODNs, **T4** and **T5**, having one or two triazolylphosphonate "caps" on both the 5′- and the 3′ ends respectively. Unmodified polythymidylate DNA (23-mer) was used as the control. The oligomers were tested for stability against snake venom phosphodiesterase (SVPDE, 3′-exonuclease) and calf-spleen phosphodiesterase (CSPDE, 5′-exonuclease).

For the SVPDE assay, a sample of the oligomer (0.7 OD) was incubated at 37 °C with 5 μg of the enzyme in Tris-HCl buffer (pH 9.0) containing 10 mM $MgCl_2$. The CSPDE assay was carried out using 0.7 OD of the oligomer and 0.1 U of the

dx.doi.org/10.1021/ja3026714 | J. Am. Chem. Soc. 2012, 134, 11618−11631

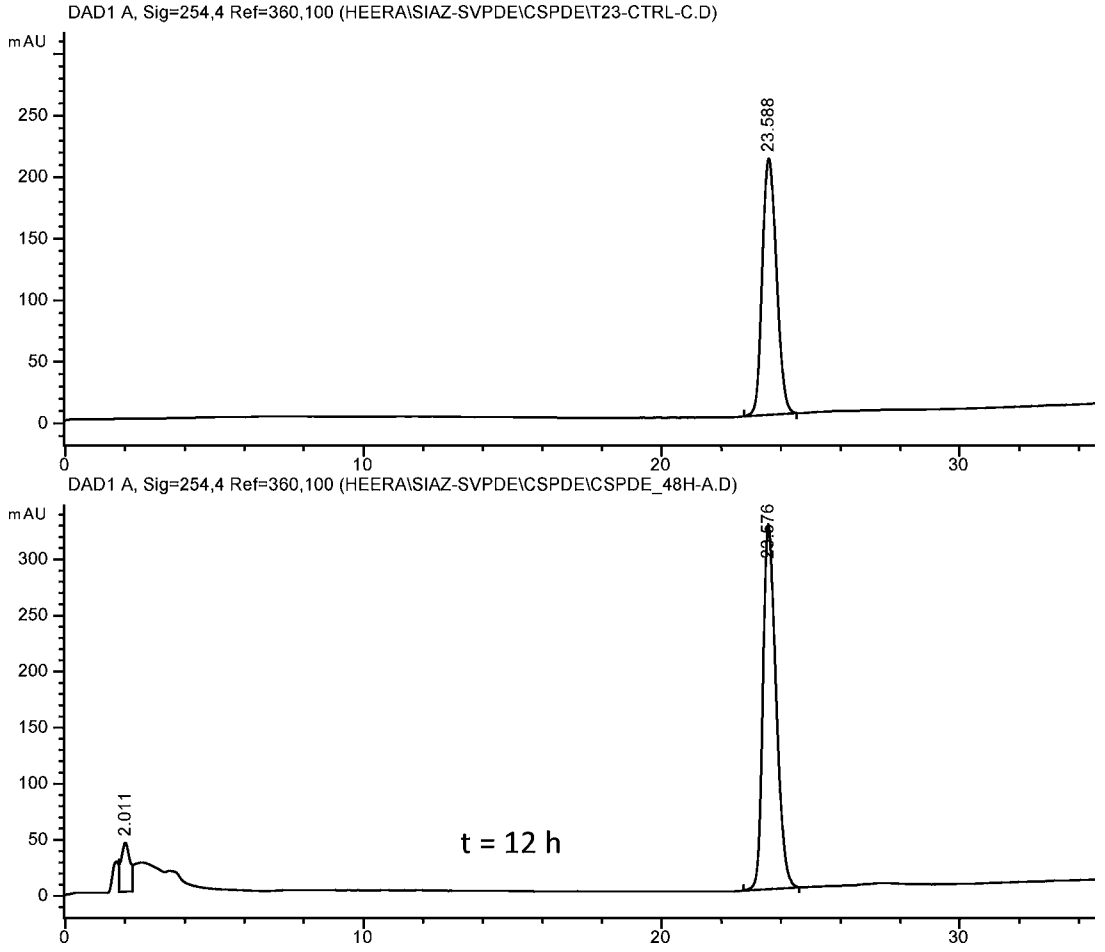

Figure 3. Time-dependent enzymatic hydrolysis of ODN **T4** in the presence of CSPDE.

Table 2. T_m Data for ODN/RNA Duplexes

		number and type of modifications						
name[a]	duplex[b]	TP linkages	2′-OMe	LNA	Thio	T_m[c] (°C)	ΔT_m[d] (°C)	ΔT_m′[e] (°C)
ODN 1	1/15	5	0	0	0	39.5	7	–
ODN 2	2/15	6	0	0	0	43.9	2.6	–
ODN 3	3/15	6	0	0	0	41.6	4.9	0.8
ODN 4	4/15	5	17	0	0	55.2	10.7	−0.4
ODN 5	5/15	6	16	0	0	51.5	14.4	−0.3
ODN 6	6/15	0	16	0	0	53.1	12.8	–
ODN 7	7/15	4	12	0	4	60	5.9	–
ODN 8	8/15	6	16	0	4	59	6.9	−0.5
ODN 9	9/15	0	16	0	4	62.1	3.8	–
ODN 10	10/15	4	0	2	0	50.4	−3.9	–
ODN 11	11/15	5	0	2	0	47.6	−1.1	−0.8
ODN 12	12/15	0	0	2	0	51.6	−5.1	–
ODN 13	13/15	5	0	5	0	69.5	−23	−0.9
ODN 14	14/15	0	0	5	0	74	−27.5	–
–	15′/15	0	0	0	0	46.5	–	–
–	16/15	0	0	0	0	65.9	–	–

[a]ODNs **1**−**14** are defined in Table 1. [b]**15** = 5′-UAG CAG CAC AUC AUG GUU UAC A-3′; **15**′ = 5′-TGT AAA CCA TGA TGT GCT GCT A-3′; **16** = 5′- UGU AAA CCA UGA UGU GCU GCU A-3′(**15**′ is DNA, **15** and **16** are RNA). [c]All T_m's represent an average of at least three experiments; [d]ΔT_m represents T_m unmodified control − T_m ODN. [e]ΔT_m′ represents the ΔT_m per modification: (T_m modified control − T_m ODN)/number of modifications.

enzyme in ammonium acetate buffer (pH 6.8) containing 2.5 mM EDTA at 37 °C. Aliquots from both reactions were removed at various times, denatured and analyzed by RP-HPLC as detailed in the SI. The half-lives were roughly based upon the time for 50% degradation (area under the peak) of the ODNs as observed by RP-HPLC. ODN **T4** with one

dx.doi.org/10.1021/ja3026714 | J. Am. Chem. Soc. 2012, 134, 11618−11631

triazolylphosphonate at the 5′ and the 3′ ends had a half-life of ∼2.5 h with SVPDE (Figure 2). A rapid degradation of internal phosphodiester linkages was anticipated once the TP cap had been removed by the enzyme. This was because the unmodified DNA control degraded in less than 5 min under the same experimental conditions. ODN **T5** with two TP modifications on each end was found to be more stable than ODN **T4**, with an approximate half-life of 3.5 h. With CSPDE, even a single modification at each end (ODN **T4**) prevented degradation of the vicinal phosphodiester linkages. Less than 20% degradation of ODN **T4** was observed even after 12 h (Figure 3). The unmodified DNA control was fully degraded by CSPDE in less than 20 min under the same conditions.

Thermal Denaturation Studies. The biological potency of an antisense ODN or an antagomir is influenced significantly by its ability to bind target RNA with high specificity under physiological conditions.[63] Because 1,2,3- triazoles are heteroaromatic, they have the ability to engage in hydrophobic interactions with nucleobases. For example, Kocalka et al. have shown that stacking four consecutive 1,2,3-triazole modifications within the major groove of a DNA−RNA duplex enhances its thermal stability by +4.3 °C per modification.[64] Interestingly, a polythymidylate decamer of ^{TL}DNA (all internucleotide phosphodiester linkages substituted by 1,2,3-triazoles) was shown to have a T_m that was higher than the unmodified DNA/DNA control by >30 °C. This effect was attributed to the complete charge neutralization of the phosphate backbone and retention of six-bond periodicity in ^{TL}DNA.[20]

In order to quantify contributions of TP linkages toward duplex hybridization, we studied the thermal denaturation characteristics of a series of triazolylphosphonate linked ODNs **1**−**14** (miR-15b antagomirs, Table 1) with the miR-15b RNA comprising the sequence 5′-UAGCAGCACAUCAUGGUUUACA-3′. Each ODN was mixed with mir-15b RNA in a 1:1 ratio at low salt conditions (10 mM sodium phosphate, 10 mM NaCl, pH 7.1) to obtain an overall concentration of 0.4 A_{260} units of the duplex. The samples were heat denatured at 85 °C for 10 min, cooled to 15 °C at a rate of 1 °C/min, and maintained at this temperature for 10 min. Melting was performed by heating the duplexes from 20 to 85 at 1 °C/min with the absorbance (260 nm) being recorded at one min intervals. Melting temperatures (T_m) were determined at the maximum of first derivative plots.

For ODNs having TP/phosphate backbones (Table 1, ODNs **1**−**3**), and ODN **11** with TP/phosphate linkages and two LNAs, the ΔT_m (Table 2) was calculated as the difference of melting temperatures of the ODN/RNA duplex and that of a DNA/RNA control duplex 15′/15. For TP/phosphate/LNA ODNs with five LNA (ODN **13**) and all TP/2′-OMe ribonucleoside ODNs (ODNs **4**-**9**), the control was an RNA/RNA duplex (16/15) as ODNs with many LNA and 2′-OMe ribonucleoside modifications usually generate A-form helices.

In order to discount the effect of modifications other than TP (LNA nucleosides, 2′-OMe ribonucleosides, thiophosphate internucleotide linkages) on the T_m of an ODN, control ODNs with the above modifications but devoid of TP linkages (**6**, **9**, **12**, and **14**) were synthesized (Tables 1, 2). These controls were used to determine the $\Delta T_m'$, which is defined as the ΔT_m per modification after discounting the effect of other modifications. It was calculated as the difference of the T_m of the antagomir/RNA duplex and the corresponding control/RNA duplex (depending on the modifications involved), divided by the number of TP modifications.

The $\Delta T_m'$ was determined in order to provide a rough estimate of the ΔT_m for the TP linkage after approximately discounting the effect of the other modifications on the duplex stability. The $\Delta T_m'$ has been calculated only for those full length ODNs that have corresponding controls. All ODN duplexes showed an increase in A_{260} upon increasing temperature and gave the characteristic sigmoidal melting curve. As anticipated, the 16-mer ODN **1** (5 TP linkages) with a truncation of 5 nucleotides from the 5′ end of the antagomir showed the lowest T_m when hybridized with complementary RNA (ΔT_m = 7 °C). For ODNs **2** and **3** with six TP linkages, the ΔT_m was 0.6−0.8 °C per modification. The slightly lower T_m observed in the case of ODN **3** (TP caps at 5′-and 3′ end) when compared to ODN **2** (TP linkages toward the center of the strand) suggests that the positioning of the TP linkages along the strand could affect hybridization stability. The 2′-OMe ribonucleoside containing ODNs (five or six TP linkages, **4**, **5**) showed only ∼0.3−0.4 °C depression per modification. This modest reduction can be attributed to the well-known fact that T_m depression can be partially offset by 2′-OMe sugar residues in a molecule[65](ODNs **4** and **5** have 17 and 16 2′-OMe ribonucleosides each). Although the introduction of thiophosphate linkages generally lower the melting temperature of 2′-deoxyoligonucleotides by about 0.6 °C per linkage,[66] a depression of 0.5 °C per TP modification (ΔT_m') was observed for ODN **8** which contained four thiophosphates in addition to the sixteen 2′-OMe ribonucleosides. The hybridization affinity improved dramatically when LNA nucleosides were added to the construct.[67] Thus, for an 18-mer ODN **10** having 2 LNA nucleosides and 4 TP linkages, the T_m was higher than for the unmodified DNA/RNA control duplex (∼4 °C). A further increase in T_m ($|\Delta T_m|$ = 27.5 °C) resulted when 5 LNA nucleosides were present (ODN **13**, five TP linkages). Discounting the positive effect of the LNA, the $\Delta T_m'$ value of a TP linkage as calculated using ODN **13** is 0.9 °C. Thus, as is the case with most phosphate backbone modifications, a triazolylphosphonate linkage slightly destabilizes the duplex when incorporated into a DNA and hybridized to complementary RNA. Since the triazolyl moiety is directly linked to the phosphorus backbone, we presume that the heteroaromatic triazole ring is not available for stacking interactions with the nucleobases during duplex formation. Whether the incorporation of a flexible spacer arm between the phosphorus atom and the 1,2,3-triazole would enhance duplex stabilization remains to be investigated. Molecular modeling simulations of twisted, intercalated nucleic acids (TINA) (the phosphorus is tethered via an 8−10 carbon spacer to the N^1-pyrenyl-1,2,3-triazole moiety) showed that only the pyrenyl fragment was engaged in stacking interactions with the nucleobases of a DNA/DNA duplex.[68]

Biological Activity of 1,2,3-Triazolylphosphonates. In a manner similar to peptidomimetics, the triazole moiety has been widely studied as a pharmacophore,[69] and several molecules with the 1,2,3-triazole core are in the final stages of clinical trials as anticancer, antibacterial, and antifungal agents.[24,70] Moreover, the pharmacokinetics of triazole based drugs have been carefully studied.[71] Given the vast literature on the biocompatibility of these molecules and our own data on the thermal and enzymatic stability of TP-modified ODNs, we were motivated to explore the cellular uptake and subcellular localization patterns of these ODNs.

It is well-known that oligonucleotide−cation conjugates possess superior cellular uptake properties and facilitate endosomal release via the proton sponge mechanism.[72,73] Since trimethylaminoethyl side chains can be easily appended to the triazolyl moiety using the Click approach,[74] we synthesized ODNs **17**−**20** carrying increasing numbers of this positively charged side chain, and compared their uptake properties with those of unsubstituted triazolylphosphonate modified ODNs **21** and **22** (Table 3). A 5′-fluorescein tag was introduced on each ODN in order to monitor cellular uptake. This tag was linked through a thiophosphate to the ODN in order to increase resistance toward degradation by nucleases.

Table 3. ODNs Used for Flow Cytometry[a]

no.	ODN
17	5′-F_s-$T^{\dagger}A_pA_pC_pA_pC_pG_pA_pT_pA_pC_pG_pC_pG_pA_pT$-3′
18	5′-F_s-$T^{\dagger}A_pA_pC_pA_pC_pG_pA_pT_pA_pC_pG_pC_pG_pA^{\dagger}T$-3′
19	5′-F_s-$T^{\dagger}A^{\dagger}A_pC_pA_pC_pG_pA_pT_pA_pC_pG_pC_pG^{\dagger}A^{\dagger}T$-3′
20	5′-F_s-$T^{\dagger}A^{\dagger}A^{\dagger}C_pA_pC_pG_pA_pT_pA_pC_pG_pC^{\dagger}G^{\dagger}A^{\dagger}T$-3′
21	5′-F_s-$T_aA_pA_pC_pA_pC_pG_pA_pT_pA_pC_pG_pC_pG_pA_aT$-3′
22	5′-F_s-$T_aA_aA_pC_pA_pC_pG_pA_pT_pA_pC_pG_pC_pG_aA_aT$-3′

[a]Superscript "†" represents the 1-trimethylaminoethyl-1,2,3-triazolyl-phosphonate linkage and subscript "a" represents the 1,2,3-triazolylphosphonate linkage; Fs represents a fluorescein tag coupled to the ODN via a thiophosphate linkage.

Flow Cytometry. Preliminary studies on the cell uptake of ODNs **17**−**22** were carried out on HeLa cells and the results quantified by fluorescence assisted cell sorting (FACS). Exponentially growing HeLa cells maintained as subconfluent monolayers in Dulbecco's Modified Eagle Medium (DMEM) were seeded on 12-well culture plates 24 h before transfection. For transfection, the medium was replaced with Opti-MEM (reduced serum medium, Gibco) premixed with the ODNs at various concentrations (0.5, 1.0, and 3.0 μM) and the cells were incubated for 16 h. The cells were then rinsed three times with D-PBS (Dulbecco's phosphate buffer saline), trypsinized, and resuspended in D-PBS. Fluorescence intensity was analyzed for cells presenting higher fluorescence than the background. The background was defined as the autofluorescence of cells incubated only with Opti-MEM (no ODN) during the 16 h transfection. Single-stranded 5′-fluorescein-labeled DNA having the same sequence was used as control. The results are shown in Chart 1.

Flow cytometry indicates that these ODNs are efficiently taken up by cells without transfecting agents and that increased uptake was dose dependent. However increasing the number of modifications beyond four did not improve cellular uptake. At 0.5 μM, ODNs **18**−**20** had comparable (30−36%) uptake. However, ODNs **21** and **22**, without positively charged side chains, had considerably higher (56%) uptake at 0.5 μM than was observed for ODNs **18** and **19** which had the same number and similar sites modified with the cationic trimethylaminoethyl group. Even though the cellular uptake mechanism of the triazolylphosphonate linkage is unknown, this preliminary study suggests that the effect of positive charges on a TP-modified backbone might be important only when the number of positive charges far exceeds the negative charges on the backbone. This conclusion is supported by recent literature which shows that the selective introduction of cationic trimethylammonium groups onto a polysaccharide (chitosan) using Click chemistry resulted in improved cellular uptake of the polymer only at nitrogen/phosphorus ratios (N/P) of 10/1.[75] Interestingly, for TP-modified ODNs, excellent cellular uptake was observed even when the strand had only 13% TP linkages (ODN **21**).

Further studies with ODNs carrying increasing number of triazolylphosphonate linkages showed that the optimum cellular uptake was observed for ODNs carrying four TP linkages (27% modified). A further increase to 40% modification did not show any enhancement in uptake efficiency. Increasing the ODN concentration in the transfection media (ODN conc. > 6.0 μM) did not result in a further shift of the fluorescence intensity peak during flow cytometry. Thus the uptake pathway appeared to be saturable at higher concentrations which suggest that receptor-mediated endocytosis might be involved.[76] Cells treated with unmodified DNA exhibited very weak fluorescence at all concentrations studied.

Fluorescence Microscopy. It is well-known that some chemically modified ODNs such as methylphosphonates and phosphorothioates adhere to cell membranes and that the amount of cell-associated fluorescence observed by FACS might not accurately reflect cell-internalized ODNs.[76,77] Hence, we investigated the subcellular distribution pattern of fluorescently labeled ODN **22** on four different cell lines using fluorescence microscopy.

HeLa, WM-239A, Jurkat and SK-N-F1 cells were incubated with 6.0 μM fluorescein tagged ODN **22** for 20 h in the absence of transfecting agents. The adherent cells (HeLa, WM-

Chart 1. Bar Diagram Showing the Percentage of HeLa Cells with Uptake, at Various Concentrations, of ODNs 17−22 after 16 h of Transfection in Opti-MEM (reduced serum medium)

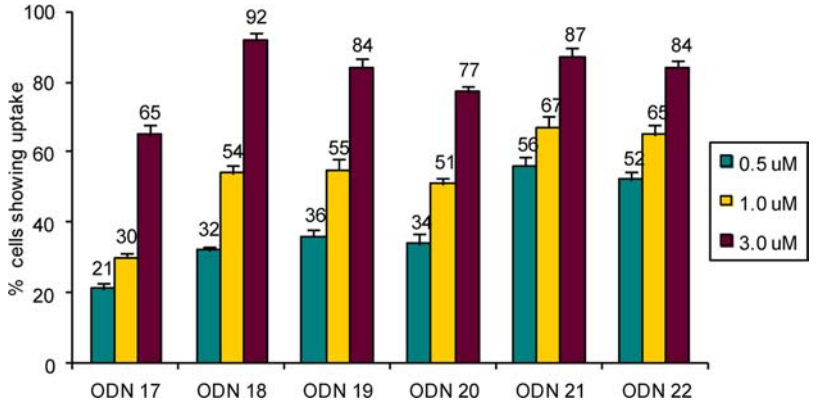

dx.doi.org/10.1021/ja3026714 | J. Am. Chem. Soc. 2012, 134, 11618−11631

239A, SK-N-F1) were then repeatedly washed with D-PBS and fixed with formalin and prepared for analysis as described in the Experimental Section. Jurkat cells were pelleted and resuspended three times with D-PBS and fixed with formalin before analysis.

We observed that the subcellular localization pattern of ODN **22** was highly dependent on cell type. In HeLa cells, the ODNs were localized predominantly in the nucleus (Figure 4A–D). In

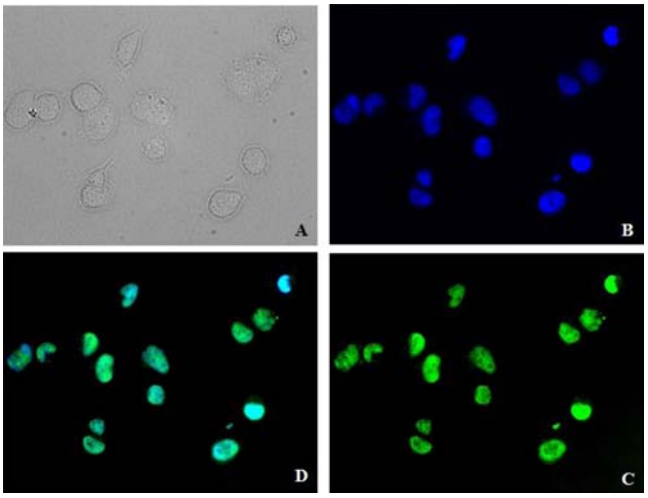

Figure 4. A. Visualization of TP ODN uptake and intracellular trafficking by fluorescence microscopy. Fluorescein labeled ODN **22** (6.0 μM in reduced serum medium (Opti-MEM)) was transfected into HeLa cells followed by 20 h of incubation at 37 °C after which the cells were washed with PBS and fixed using buffered formalin solution. Nuclei of the cells were counterstained with DAPI (blue). Phase contrast image (40×) of HeLa cells. **B**. Image showing the DAPI nuclear localization of the same cells. **C**. Image showing fluorescein localization. **D**. Image showing the merge of images **B** and **C**.

WM-239A cells, localization was found to be highly diffuse in the cytoplasm with little or no nuclear uptake. In addition to being highly diffuse, the cytoplasmic fluorescence was not punctuated or granular (Figure 5A–D). Since the ODN does not appear to be sequestered in endosomal compartments, it is anticipated that it might be readily available for biological activity in the cytoplasm of these cells. In Jurkat cells, the fluorescence was both punctate and diffuse while being located primarily in the cytoplasm (Figure 6A–D). Given the inherently poor transfection efficiency observed in neuroblastoma cell lines,[78] we were encouraged by the finding that ODN **22** was taken up by the SK-N-F1 cell line (human neuroblastoma; Figure 7A–D). In these cells, the subcellular distribution appeared to be predominantly cytoplasmic. A literature search for similar findings revealed that nuclear localization was observed when HeLa cells were transfected with fluorescein labeled, polyimidazole conjugated deoxyoligonucleotides (6 histamine residues, T_{12}). The uptake was found to proceed via active transport followed by membrane destabilization.[79] Imidazole containing polymers have also been explored as effective gene delivery agents because of their ability to release cargo into the cytoplasm via endosomolysis.[80]

It is interesting that the localization of the synthetic ODN was highly dependent on cell types. However, a simple explanation to this phenomenon is currently unavailable. The subcellular distribution might vary depending on the internal-

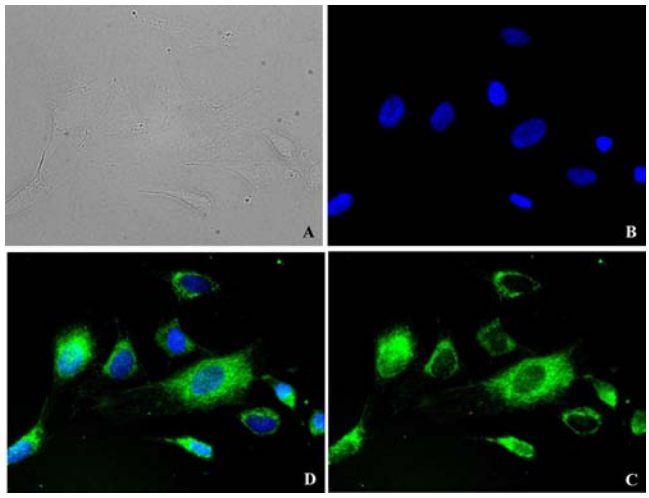

Figure 5. Visualization of TP ODN uptake and intracellular trafficking by fluorescence microscopy. Fluorescein labeled ODN **22** (6.0 μM in Roswell Park Memorial Institute Medium, RPMI) was transfected into WM-239A cells followed by 20 h of incubation at 37 °C. They were then washed with PBS and fixed using buffered formalin solution. Nuclei of the cells were counterstained with DAPI (blue). **A**. Phase contrast image (40X) of WM-239A cells. **B**. Image showing the DAPI nuclear localization of the same cells. **C**. Image showing fluorescein localization. **D**. Image showing the merge of images **B** and **C**.

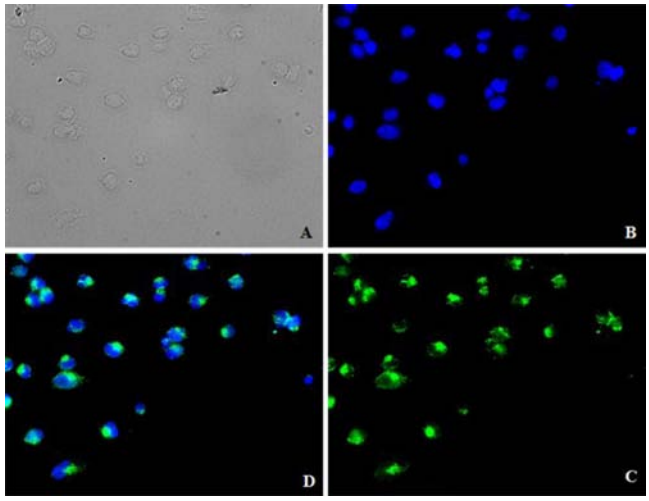

Figure 6. Visualization of TP ODN uptake and intracellular trafficking by fluorescence microscopy. Fluorescein labeled ODN **22** (6.0 μM in RPMI) was transfected into Jurkat cells followed by 20 h of incubation at 37 °C. They were then washed, pelleted and resuspended in PBS, and fixed using buffered formalin solution. Nuclei of the cells were counterstained with DAPI (blue). **A**. Phase contrast image (40X) of Jurkat cells. **B**. Image showing the DAPI nuclear localization of the same cells. **C**. Image showing fluorescein localization. **D**. Image showing the merge of images **B** and **C**.

ization pathways adopted by the cell type as well as the subsequent subcellular trafficking mechanism. Many different internalization pathways for ODNs have been discovered. For instance, phagocytosis takes place only in specialized cells such as macrophages and granulocytes, while the other pathways such as clathrin or caveolin-mediated uptake, macropinocytosis, receptor mediated uptake (transferrin receptor, LDL receptor, Toll-like receptors), are predominant in other cell types.[81] Once the ODN enters the cell by one of the above

dx.doi.org/10.1021/ja3026714 | J. Am. Chem. Soc. 2012, 134, 11618–11631

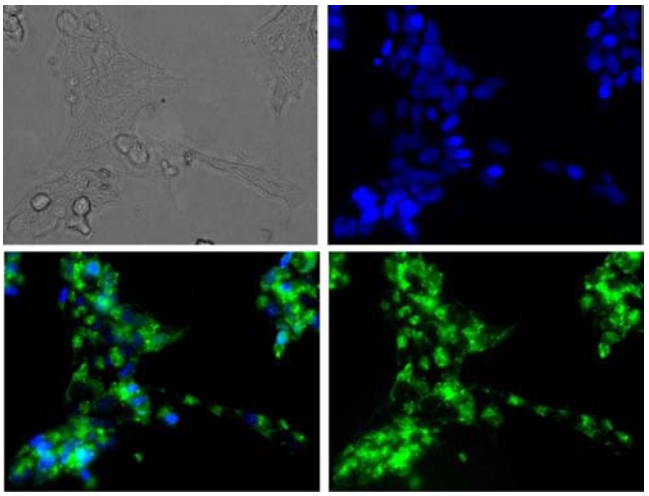

Figure 7. Visualization of TP ODN uptake and intracellular trafficking by fluorescence microscopy. Fluorescein-labeled ODN **22** (6.0 μM in reduced serum medium (Opti-MEM)) was transfected into SK-N-F1 cells followed by 20 h of incubation at 37 °C. They were then washed with PBS and fixed using buffered formalin solution. Nuclei of the cells were counterstained with DAPI (blue). (A) Phase contrast image 40× SK-N-F1 cells. (B) Image showing the DAPI nuclear localization of the same cells. (C) Image showing fluorescein localization. (D) Image showing the merge of images B and C.

mechanisms, it encounters a complex maze of intracellular pathways that ultimately determine its subcellular distribution pattern.[82] To the best of our knowledge, there have been no reports on the differential uptake of the same chemically modified ODN in different cell types. However, a search for parallels in the literature reveals that the subcellular localization patterns of the well-studied phosphorothioate oligonucleotides (PS-ODNs) vary depending on cell type. Nuclear localization was observed in bovine adrenal cortex cells,[83] but in K562 human leukemia cells, these ODNs were localized within or at the periphery of endosomes, and were also visualized free within the cytoplasm and within the nucleus.[84] In human keratinocytes, PS-ODNs assumed a punctate distribution in the cytoplasm with no nuclear uptake.[85] Taken together, these studies suggest that the cellular uptake and distribution pattern of ODNs depend on a multitude of factors such as the nature of the chemical modifications, the sequence and the length of the ODN, the mechanism of uptake and the internalization pathways adopted.

Currently, the internalization pathway (or pathways) adopted by triazolylphosphonate modified ODNs are unknown. Presumably, different pathways might be preferred by each cell type. Alternatively, the ODN might leak from endomembrane compartments during intracellular trafficking or facilitate either endosomal rupture or membrane fusion.[81]

Cytotoxicity Assays. For cytotoxicity experiments, ~1 × 10^5 HeLa or WM-239A cells (or ~2 × 10^5 Jurkat cells) were seeded onto 12-well plates and incubated in appropriate medium containing 10% fetal bovine serum, penicillin (100 U/mL) and streptomycin (100 U/mL) for 24 h. All three cell lines were treated with 6.0 μM ODN **22** and incubated for 20 h at 37 °C. After incubation, the cells were washed in PBS, (followed by trypsinization in the case of HeLa and WM-239A), and suspended in the Annexin-V binding buffer. Suspensions of cells were counted and adjusted to a density of 1 x10^6cells/ml. They were stained with annexin-V FITC followed by propidium iodide (PI), and then kept in the dark for 10 min and sorted by flow cytometry. Each experiment was repeated three times for statistical relevance. Cells that were not treated with ODN **22** but stained with annexin-V FITC and PI were used as the negative control. Cells stained with either annexin-V FITC or PI were used to correct for compensation. Cells that were not stained with both dyes served as controls for optimizing the voltage settings on the instrument. From these assays, we concluded that the cytotoxicity of the triazolylphosphonate ODN was negligible in all cell lines studied. The presence of copper adducts of ODNs did not show significant toxicity in these experiments. In HeLa cells, the control showed 13.7% cell death and the ODN treated sample 14.1%. With WM-239A cells, the control and ODN-treated samples showed 2.5% and 3% cell death respectively, whereas control Jurkat cells showed 8.8% cell death as opposed to 9.7% for the sample.

Since no cytotoxicity owing to the presence of the copper was detected in the cell lines tested, a literature search for studies that evaluate the extent of toxicity of copper to mammalian cells was carried out. It has been reported that in the case of PBMCs (peripheral blood mononuclear cells), the cell viability was virtually unaffected in the concentration range 0−10 μM, but a sharp decrease in viability was observed at concentrations ranging from 50−150 μM.[86] In human hepatoma cells (HepG2), exposure to >64 μM of Cu^{2+} caused up to 18% necrosis as opposed to <5% below this concentration.[87] In HeLa cells, copper ions at concentrations ranging from 1−100 μM did not interfere with cell growth although retarded cell growth was observed at 500 μM.[88] Thus, copper toxicity in mammalian cells is negligible at low concentrations up to 10 μM, and hence remained undetected in this study.

■ SUMMARY

We have prepared a new 2′-deoxynucleoside 3′-phosphoramidite synthon, the alkynylphosphinoamidite, and demonstrated that it is compatible with standard phosphoramidite chemistry. To the best of our knowledge, alkynyl phosphinoamidites are novel compounds that have not previously been synthesized. A unique feature of this chemistry is that it facilitates introduction of chemical modifications onto the DNA backbone via CuAAC at any position along the DNA strand in a sequence independent manner and allows site specific postsynthetic modifications that are incompatible with conventional DNA synthesis reagents. Postsynthetic conjugation on the solid-phase also has the advantage that excess reagents can be used to drive the reaction to completion. Moreover, this chemistry can be tailored so as to develop a 5′-terminating ligand which can "Click" two molecules of interest together, or to introduce multiple Click reactions[89] onto an ODN. Using this chemistry, chimeric triazolylphosphonate modified ODNs having phosphates and thiophosphate internucleotide linkages, LNA nucleosides, and 2′-OMe ribonucleosides (16−23 mers) have been synthesized in good yields. A single TP modification at the 3′- and 5′-ends generated an oligomer that was approximately 30 times more stable than native DNA toward SVPDE digestion. A 40-fold increase in nuclease resistance toward CSPDE was also observed. This exceptional stability could be partially attributed to the P−C bond. The absence of triazoles in biological systems might also contribute to nuclease stability as they may not be recognizable by nucleases. Although this linkage is nonionic and can engage in hydrogen-bonding interactions, TP-modified ODNs displayed a mild helix

dx.doi.org/10.1021/ja3026714 | J. Am. Chem. Soc. 2012, 134, 11618−11631

destabilizing effect when hybridized to complementary RNA. This effect might be due to the steric bulk of a rigid triazolyl moiety which could pucker the sugar−phosphate backbone into an energetically unfavorable conformation. Alternatively, one diastereomer of the triazolylphosphonate could be destabilizing toward double helix formation. Presumably, the ODN-bound copper impurity might also exert a minor influence on T_m values, depending on whether it is bound to the phosphate or the nucleobase. Fluorescence microscopy revealed that TP-modified ODNs are taken up, in the absence of cationic lipids, by difficult-to-transfect cell lines (Jurkat, SK-N-F1) and that the fluorescence intensities observed by FACS does not arise from membrane-bound ODNs. The most intriguing observation however was the differential uptake of the same ODN by various cell types. While the fluorescence was predominantly nuclear in HeLa cells, a diffuse cytoplasmic distribution was observed in the WM-239A cell line. A mechanistic study might provide valuable insights into the highly efficient uptake pathway of these ODNs even when the oligonucleotide is only 27% modified. It remains to be seen whether nuclear uptake will be observed in other cell types and if this observation can be exploited for designing efficient antisense or antigene agents that require nuclear localization. Perhaps as well, the observation that certain cell lines localize these ODNs almost exclusively in the cytoplasm may facilitate the use of antagomirs where cytoplasmic distribution is necessary. Future research will address important challenges concerning the effective design of potent siRNAs and antagomirs having the TP linkage as well as efficient targeted delivery of these ODNs in vivo.

■ CONCLUSION

In summary, we have developed new phosphoramidite synthons of all four bases (A, G, C, and T) that can be used in conjunction with CuAAC reaction for the site-specific backbone modification of DNA. Our methodology enables the multiple, high-density functionalization of the phosphorus backbone of an oligodeoxynucleotide using Click chemistry. Given the versatility of the CuAAC reaction, various biologically relevant moieties, labeling dyes, diagnostic elements etc. can be introduced at the phosphorus center as opposed to the bases. This is advantageous because the base-pairing ability of the DNA will not be significantly altered which makes this the method of choice for adding desirable properties onto a DNA strand without compromising their hybridization ability. The ODNs generated by this strategy were found to be highly stable to nucleases and displayed excellent cell uptake properties without the aid of transfection agents. Subcellular distribution patterns of the ODN were found to be highly dependent on cell type. Taken together, these studies demonstrate that triazolylphosphonate-modified ODNs are ideal candidates for studying gene silencing and RNAi.

■ EXPERIMENTAL SECTION

Chemical Synthesis. *Synthesis of Bis(N,N-diisopropylamino)-ethynylphosphine (5).* To a flame-dried 500-mL Schlenk flask equipped with a magnetic stir bar and septum under nitrogen was added 0.02 mols of bis(*N*,*N*-diisopropylamino) chlorophosphine. Anhydrous diethyl ether (350 mL) was added and the mixture was cooled with stirring, to 0 °C. To this solution, ethynylmagnesium bromide (0.5 M in THF, 1.1 equiv) was added dropwise via a syringe over a period of 15 min, and the reaction mixture was allowed to stir at 0 °C for one hour. The ^{31}P NMR spectrum after one hour indicated complete conversion of the starting material to product. The reaction mixture was allowed to attain room temperature, filtered under nitrogen, and concentrated on a rotary evaporator. The resulting viscous oil was extracted three times with anhydrous hexanes during which the oil transformed into a solid. The solid was dissolved in a minimum volume of anhydrous acetonitrile, and this solution was extracted twice with anhydrous hexanes. All hexane fractions were combined and concentrated in vacuo to give a translucent white oil, which was found to be >99% pure by ^{31}P NMR spectroscopy.Yield: 90%; ^{1}H NMR ($CDCl_3$): δ 3.53 (m, 4H), 3.02 (d, 1H), 1.19, 1.18 (d, 12H) and 1.17, 1.16 (d, 12H). ^{31}P NMR ($CDCl_3$): δ 28.0 (s). ^{13}C NMR ($CDCl_3$): δ 68.1, 65.7, 25.9, 14.8.

The general procedure for the synthesis of 5′-*O*-dimethoxytrityl-2′-deoxyribonucleoside 3′-*O*-ethynylphosphinoamidites (**6**−**9**, Scheme 1) is as follows: Appropriately base-protected 5′-*O*-dimethoxytrityl-2′-deoxyribonucleosides (**1**−**4**) (0.02 mols, 1.0 equiv), 1*H*-tetrazole (0.03 mol, 1.5 equiv) and anhydrous dichloromethane (100 mL) were taken up in a 250 mL round-bottom flask and stirred under nitrogen until the 2′-deoxyribonucleoside dissolves completely. Anhydrous dichloromethane (250 mL), bis(*N*,*N*-diisopropylamino)ethynylphosphine (**5**) (0.02 mol, 1.0 equiv), and a magnetic stir bar were placed in a 500 mL round-bottom flask fitted with a 150 mL addition funnel. The freshly prepared solution of 2′-deoxyribonucleoside and 1*H*-tetrazole was taken up in the addition funnel and added slowly over 30 min to the 500 mL round-bottom flask containing (**5**) under nitrogen. The mixture was allowed to stir for an additional 30 min. Triethylamine (approximately 0.2 mL) was added to neutralize the solution and the solvent was removed in vacuo. The crude product was isolated by chromatography using a 30−90% gradient of ethyl acetate in hexane containing 1% triethylamine.

*Compound **6**. 5′-O-Dimethoxytrityl-N^6-tert-butylphenoxyacetyl-2′-deoxyriboadenosine 3′-O-ethynylphosphinoamidite:* Yield: 66%; ^{31}P NMR ($CDCl_3$): δ 97.9, 96.4; ^{1}H NMR ($CDCl_3$): δ 8.74 (s, 1H), 8.24 (s, 1H), 7.40−7.18 (m, 10H), 7.02−6.78 (m, 7H), 5.32 (s, 1H), 4.84 (s, 1H), 4.34 (m, 1H), 3.79 (s, 6H), 3.42 (m, 2H), 3.07 (d, 1H), 2.71−2.61 (m, 1H), 2.06 (s, 1H), 1.32 (s, 9H), 1.22−1.19 (m, 12H). ^{13}C NMR ($CDCl_3$): δ 166.8, 158.5, 154.5, 152.4, 147.9, 135.6, 130.0, 127.8, 126.6, 114.5, 113.1, 91.5, 84.4, 68.3, 55.2, 34.2, 31.5, 22.6.

*Compound **7**. 5′-O-Dimethoxytrityl-N^2-tert-butylphenoxyacetyl-2′-deoxyriboguanosine 3′-O-ethynylphosphinoamidite:* Yield: 50%; ^{31}P NMR ($CDCl_3$): δ 97.3, 96.3; ^{1}H NMR ($CDCl_3$): δ 7.93 (s, 1H), 7.23−6.73 (m, 17H), 6.31 (t, 1H), 5.29 (s, 2H), 4.64 (s, 2H), 4.29 (m, 1H), 3.77 (s, 6H), 3.30 (m, 2H), 3.06 (d, 2H), 2.61 (m, 2H), 2.04 (s, 1H), 1.33 (s, 9H), 1.21−1.12 (m, 12H). ^{13}C NMR ($CDCl_3$): δ 168.3, 161.5, 158.2, 154.1, 145.8, 144.2, 130.4, 127.7, 126.8, 112.7, 92.4, 87.7, 87.4, 67.9, 65.4, 55.2, 31.4.

*Compound **8**. 5′-O-Dimethoxytrityl-N^4-tert-butylphenoxyacetyl-2′-deoxyribocytidine 3′-O-ethynylphosphinoamidite:* Yield: 55%; ^{31}P NMR ($CDCl_3$): δ 100.2, 96.6; ^{1}H NMR ($CDCl_3$): δ 9.10 (s, 1H), 8.39 (d, 1H) 8.27 (d, 1H), 7.43−7.25 (m, 10H), 6.88−6.82 (m, 7H), 4.58 (s, 2H), 3.80 (s, 6H), 3.49 (s, 1H), 3.47 (s, 1H), 3.04 (d, 2H), 2.99 (d, 2H), 2.82 (m, 2H), 2.33 (m, 2H), 2.04 (s, 1H), 1.30 (s, 9H), 1.19−1.16 (m, 12H). ^{13}C NMR ($CDCl_3$): δ 169.6, 158.6, 155.3, 154.2, 147.7, 145.9, 144.4, 136.9, 130.3, 128.1, 127.9, 126.9, 114.4, 92.1, 86.5, 83.7, 67.1, 63.5, 55.2, 53.4, 34.3, 31.4.

*Compound **9**. 5′-O-Dimethoxytrityl-2′-deoxyribothymidine 3′-O-ethynylphosphinoamidite:* Yield: 45%; ^{31}P NMR ($CDCl_3$): δ 98.35, 96.20; ^{1}H NMR ($CDCl_3$): δ 7.63 (s, 1H), 7.60 (d, 2H), 7.30−7.23 (m, 10H), 6.83 (d, 2H), 6.47 (t, 1H), 6.38 (t, 1H), 4.66 (t, 1H), 4.16−4.10 (m, 1H), 3.90−3.87 (m, 1H), 3.78 (s, 6H), 3.33 (m, 3H), 3.04 (d, 2H), 2.60−2.46 (m, 1H), 2.33 (m, 2H), 2.04 (s, 3H), 1.25−1.06 (m, 18H). ^{13}C NMR ($CDCl_3$): δ 163.8, 158.5, 150.7, 143.9, 137.6, 136.2, 129.3, 128.4, 126.3, 114.6, 111.3, 78.8, 77.4, 63.6, 55.8, 45.9, 38.4, 22.4, 15.7.

Solid-Phase Synthesis. Solid-phase synthesis was carried out using an ABI model 394 automated DNA synthesizer. The synthetic protocol (SI, Table S1) was based on the conventional DMT-phosphoramidite method. The 5′-O-dimethoxytrityl-2′-deoxyribonucleoside 3′-*O*-ethynylphosphinoamidites (**6**−**9**) were used for coupling in positions where triazolylphosphonate modification was necessary. To generate 2′-deoxyribonucleoside phosphate linkages, commercially

available ultramild 5′-O-dimethoxytrityl-3′-*O*-cyanoethylphosphoramidites 2′-deoxyribonucleosides of A, G, C, and T were purchased from ChemGenes (MA) and used without further purification. 5′-*O*-Dimethoxytrityl-LNA nucleoside 3′-*O*-cyanoethylphosphoramidites were obtained from Exiqon (UK). Commercially available ultramild 5′-*O*-dimethoxytrityl-2′-OMe ribonucleoside 3′-*O*-cyanoethylphophoramidites of A, G, C, and U were purchased from Glen Research (VA). All appropriately protected deoxyribo and ribonucleoside 3′-*O*-cyanoethylphosphoramidites were dissolved in anhydrous acetonitrile at a concentration of 100 mM and placed on the appropriate ports of the synthesizer. Prior to synthesis, the 5′-DMT group on the support-bound 2′-deoxyribonucleoside was removed with 3% dichloroacetic acid in dichloromethane. The coupling wait time was 600 s for the 5′-*O*-dimethoxytrityl-2′-deoxyribonucleoside 3′-*O*-ethynylphosphinoamidites (**6**–**9**). All commercially available deoxyribo and ribonucleoside phosphoramidites were used according to the manufacturer's recommendations. The activator was 5-ethylthio-1*H*-tetrazole (0.25 M in anhydrous acetonitrile, Glen Research, VA). After each condensation step, the support was washed with acetonitrile for 40 s and Unicap phosphoramidite (Glen Research, VA) was used according to the manufacturer's recommendations for capping failure sequences. The standard oxidation reagent (0.02 M iodine in THF/water/pyridine) was used for oxidation. Beaucage Reagent dissolved in acetonitrile (1 g/100 mL) was used to generate thiophosphate linkages. This cycle was repeated until the ODN of the desired sequence and length was synthesized. Postsynthesis the CPG linked to the ODN was removed from the column and placed in a 1.5 mL screw cap, conical glass reaction vial. The Click reaction was carried out using an appropriate azide (See SI). A heterogeneous mixture of the solid-support bound ethynylphosphonate ODN, the azide, $CuSO_4 \cdot 5H_2O$, sodium ascorbate, and TBTA (1:6:0.8:6:7 molar equiv. respectively) in water/methanol/THF (1.2 mL, 2:2:1 v/v/v) was allowed to react at room temperature for 7 h in order to obtain the respective triazolyl phosphonate ODN. The support was then washed successively with water (2 × 20 mL) followed by methanol (2 × 10 mL), acetonitrile (2 × 10 mL) and dichloromethane (2 × 10 mL). After drying the support, a 50% solution of anhydrous ethylenediamine in toluene was added. The vial was vortexed in order to stir the contents, and cleavage of the ODN from the support was allowed to proceed for 2.5 h at room temperature. The cleavage mixture was discarded and the solid-support was evaporated to dryness in a SpeedVac. The ODN product adsorbed on the support was dissolved in 5% acetonitrile–water and purified by RP-HPLC.

Nuclease Stability Experiments. Snake venom phosphodiesterase I and calf spleen phosphodiesterase II were purchased from Sigma (St. Louis, MO). While performing enzymatic hydrolysis experiments, 10 μL of 1 M Tris buffer, 10 μL of 0.1 M $MgCl_2 \cdot 6H_2O$, ODN T4 or T5 (0.7 OD) and snake venom phosphodiesterase (5 μg) were mixed and the total volume made up to 100 μL; 20 μL aliquots of the reaction mixtures were removed at the indicated time points, quenched by the addition of 1.0 M EDTA, and stored in dry ice until analyzed by analytical RP-HPLC. For the CSPDE assay, 5 μL of 5 M ammonium acetate buffer (pH 6.8), 2.5 mM EDTA (38 μL), ODN T4 or T5 (0.7 OD) and 0.07 U of CSPDE were mixed and made up to a total volume of 100 μL. Twenty microliter aliquots of the reaction mixtures were removed at the indicated time points, quenched by the addition of 2.0 M urea and stored in dry ice until analyzed by analytical RP-HPLC.

Preparation of Cells. HeLa cells, Jurkat cells, and SK-N-F1 cells were obtained from American Type Culture Collection (Rockville, MD) and serially maintained at monolayer cultures in a humidified atmosphere of 5% carbon dioxide at 37 °C in Dulbecco's Modified Eagle's Medium (HeLa, SK-N-F1) and Roswell Park Memorial Institute Medium (WM-239A, Jurkat), containing 10% fetal bovine serum, penicillin (100 U/mL) and streptomycin (100 U/mL). They were counted and adjusted to the appropriate density, seeded onto 12-well culture plates, and incubated for 24 h prior to ODN transfection. HeLa cells were used at passages 12–18 and SK-N-F1 cells were used at passages 3–7. Jurkat cells were used at passages 7–12. The WM-239A cell line was a gift from Prof. Natalie Ahn, Department of Chemistry and Biochemistry, University of Colorado at Boulder, Boulder, CO, United States. These cells were routinely maintained as monolayers in Roswell Park Memorial Institute Medium (RPMI) containing 10% fetal bovine serum, penicillin (100 U/mL) and streptomycin (100 U/mL) and used at passages 7–10.

Transfection Experiments. For transfection experiments, ∼1 × 10^5 HeLa cells/well (12-well plates) were incubated in Dulbecco's Modified Eagle's Medium (DMEM) containing 10% fetal bovine serum, penicillin (100 U/mL) and streptomycin (100 U/mL) for 24 h. The concentration (OD) of 5′-fluorescein-labeled ODN dissolved in siRNA buffer 1× (Thermo Scientific) was measured by UV spectroscopy. The media was removed and the cells were transfected with the ODN in reduced serum medium (Opti-MEM) to give the required final concentration. The cells were then incubated at 37 °C for 16 h. After incubation, the media was removed from the wells and cells were washed three times with 0.5 mL D-PBS. Cells were then treated for 3 min at 37 °C with a prewarmed solution of trypsin–EDTA (1×) until all cells became round and detached from the plates. The cells from each plate were then taken up in 1 mL D-PBS and pelleted by centrifugation at 1000 rpm for 5 min. The pellets were washed and resuspended in D-PBS and kept at 0 °C in the dark until analyzed by flow cytometry. Jurkat cells (∼2 × 10^5 cells) were grown in suspension in 12-well plates and incubated in Roswell Park Memorial Institute Medium (RPMI) containing 10% fetal bovine serum, penicillin (100 U/mL) and streptomycin (100 U/mL) for 24 h. The cells were transfected with the ODNs and incubated at 37 °C for 16 h. After incubation, the cells were pelleted by centrifugation at 1000 rpm for 5 min, resuspended in D-PBS, and washed twice with D-PBS. The final pellet was resuspended in 100 μL of D-PBS and kept at 0 °C in the dark until used for flow cytometric analysis.

Flow Cytometry. Flow cytometric data on at least 10,000 cells per sample were acquired on a Moflow flow-cytometer (Beckman-Coulter) equipped with a single 488 nm argon laser, 530/40 nm emission filter (Fluorescein). Raw flow cytometry data were manipulated and visualized using Summit 4.3 software (Beckman-Coulter). Fluorescence intensity of the 5′-fluorescein tag was analyzed for cells presenting higher fluorescence than the background. The background was defined as the auto fluorescence of cells.

Fluorescence Microscopy. An inverted microscope (Olympus IX 81) equipped with a Hamamatsu C4742–95 CCD and CoolSNAP ES digital camera (Photometrics) was used for fluorescence microscopy. For microscopic analysis, ∼1 × 10^5 cells (HeLa, WM-239A) were seeded onto sterile coverslips (18 mm diameter, VWR) placed in 12-well plates and incubated in appropriate medium containing 10% fetal bovine serum, penicillin (100 U/mL) and streptomycin (100 U/mL) for 24 h. The cells were transfected with ODN **22** and incubated at 37 °C for 20 h. After incubation, the medium was removed from the wells and cells washed four times with 0.5 mL PBS. The cells were covered with 1 mL of 10% neutral, buffered formalin solution (Sigma-Aldrich) for 15 min. The formalin solution was removed and the cells washed, and covered with 2 mL of D-PBS for 10 min at RT. The coverslips were carefully removed from the wells and mounted upside-down on cover slides (25 × 75 mm, 1.0 mm thick) using Fluoromount-G with DAPI (Southern Biotech) as the mounting medium, and observed under the microscope.

Jurkat cells (∼2 × 10^5 cells) were seeded in suspension in 12-well plates in the absence of coverslips and incubated in RPMI containing 10% fetal bovine serum, penicillin (100 U/mL) and streptomycin (100 U/mL) for 24 h. The SK-N-F1 cell line was purchased from American Type Culture Collection (ATCC) and passaged in DMEM containing 10% fetal bovine serum, penicillin (100 U/mL) and streptomycin (100 U/mL). Prior to the fluorescence microscopy experiments, they were seeded (∼2 × 10^5 cells) onto sterile coverslips (18 mm diameter, VWR) placed in 12-well plates in appropriate culture media and incubated for 24 h. Both cell lines were transfected with ODN 22 and incubated at 37 °C for 20 h. After incubation, the cells were trypsinized, pelleted by centrifugation at 1000 rpm for 5 min, resuspended in D-PBS, and washed twice with D-PBS. The final pellet was resuspended in 100 μL of D-PBS, fixed with formalin, washed with D-PBS, pelleted, and resuspended in 100 μL D-PBS. Cells were then

dx.doi.org/10.1021/ja3026714 | J. Am. Chem. Soc. 2012, 134, 11618–11631

mounted onto cover slides using DAPI-Fluoromount G and observed under the microscope.

■ ASSOCIATED CONTENT

Supporting Information

General procedures for chemical synthesis, analytical RP-HPLC profiles of ODNs, MALDI data on select ODNs, data on PAGE, apoptosis assay protocol. This material is available free of charge via the Internet at http://pubs.acs.org.

■ AUTHOR INFORMATION

Corresponding Author

Marvin.Caruthers@colorado.edu

Notes

The authors declare no competing financial interest.

■ ACKNOWLEDGMENTS

We thank Rich Shoemaker for assistance with the NMR facility, Theresa Nahreini for FACS data collection, Prof. Natalie Ahn for the fluorescence microscope, and the University of Colorado Central Analytical Laboratories for the mass spectral facility. This research was supported by the University of Colorado at Boulder.

■ REFERENCES

(1) Keefe, A. D.; Pai, S.; Ellington, A. *Nat. Rev. Drug Discovery* **2010**, *9*, 537.
(2) El-Sagheer, A. H.; Brown, T. *Proc. Natl. Acad. Sci. U.S.A.* **2010**, *107*, 15329.
(3) Cho, Y. S.; Kim, M.-K.; Cheadle, C.; Neary, C.; Park, Y. G.; Becker, K. G.; Cho-Chung, Y. S. *Proc. Natl. Acad. Sci. U.S.A.* **2002**, *99*, 15626.
(4) Kandimalla, E. R.; Bhagat, L.; Li, Y.; Yu, D.; Wang, D.; Cong, Y.-P.; Song, S. S.; Tang, J. X.; Sullivan, T.; Agrawal, S. *Proc. Natl. Acad. Sci. U.S.A.* **2005**, *102*, 6925.
(5) Miller, M. B.; Tang, Y.-W. *Clin. Microbiol. Rev.* **2009**, *22*, 611.
(6) Seeman, N. C. *Annu. Rev. Biochem.* **2010**, *79*, 65.
(7) Kawasaki, A. M.; Casper, M. D.; Freier, S. M.; Lesnik, E. A.; Zounes, M. C.; Cummins, L. L.; Gonzalez, C.; Cook, P. D. *J. Med. Chem.* **1993**, *36*, 831.
(8) Campbell, M. A.; Wengel, J. *Chem. Soc. Rev.* **2011**, *40*, 5680.
(9) Jeong, J. H.; Mok, H.; Oh, Y.-K.; Park, T. G. *Bioconjugate Chem.* **2008**, *20*, 5.
(10) Tornøe, C. W.; Christensen, C.; Meldal, M. *J. Org. Chem.* **2002**, *67*, 3057.
(11) Rostovtsev, V. V.; Green, L. G.; Fokin, V. V.; Sharpless, K. B. *Angew. Chem., Int. Ed.* **2002**, *41*, 2596.
(12) Best, M. D. *Biochemistry* **2009**, *48*, 6571.
(13) El-Sagheer, A. H.; Brown, T. *Chem. Soc. Rev.* **2010**, *39*, 1388.
(14) Seo, T. S.; Li, Z.; Ruparel, H.; Ju, J. *J. Org. Chem.* **2002**, *68*, 609.
(15) Whiting, M.; Muldoon, J.; Lin, Y.-C.; Silverman, S. M.; Lindstrom, W.; Olson, A. J.; Kolb, H. C.; Finn, M. G.; Sharpless, K. B.; Elder, J. H.; Fokin, V. V. *Angew. Chem., Int. Ed.* **2006**, *45*, 1435.
(16) de Miguel, G.; Wielopolski, M.; Schuster, D. I.; Fazio, M. A.; Lee, O. P.; Haley, C. K.; Ortiz, A. L.; Echegoyen, L.; Clark, T.; Guldi, D. M. *J. Am. Chem. Soc.* **2011**, *133*, 13036.
(17) Lau, Y. H.; Rutledge, P. J.; Watkinson, M.; Todd, M. H. *Chem. Soc. Rev.* **2011**, *40*, 2848.
(18) Struthers, H.; Mindt, T. L.; Schibli, R. *J. Chem. Soc., Dalton Trans.* **2010**, *39*, 675.
(19) Pedersen, D. S.; Abell, A. *Eur. J. Org. Chem.* **2011**, 2399.
(20) Isobe, H.; Fujino, T.; Yamazaki, N.; Guillot-Nieckowski, M.; Nakamura, E. *Org. Lett.* **2008**, *10*, 3729.
(21) Lucas, R.; Zerrouki, R.; Granet, R.; Krausz, P.; Champavier, Y. *Tetrahedron* **2008**, *64*, 5467.
(22) El-Sagheer, A. H.; Sanzone, A. P.; Gao, R.; Tavassoli, A.; Brown, T. *Proc. Natl. Acad. Sci. U.S.A.* **2011**, *108*, 11338.
(23) El-Sagheer, A. H.; Brown, T. *Chem. Commun.* **2011**, *47*, 12057.
(24) Agalave, S. G.; Maujan, S. R.; Pore, V. S. *Chem.—Asian J.* **2011**, *6*, 2696.
(25) Kumar, R.; El-Sagheer, A.; Tumpane, J.; Lincoln, P.; Wilhelmsson, L. M.; Brown, T. *J. Am. Chem. Soc.* **2007**, *129*, 6859.
(26) Paredes, E.; Das, S. R. *ChemBioChem* **2011**, *12*, 125.
(27) Gutsmiedl, K.; Fazio, D.; Carell, T. *Chem.—Eur. J.* **2010**, *16*, 6877.
(28) Gogoi, K.; Mane, M. V.; Kunte, S. S.; Kumar, V. A. *Nucleic Acids Res.* **2007**, *35*, e139.
(29) Yamada, T.; Peng, C. G.; Matsuda, S.; Addepalli, H.; Jayaprakash, K. N.; Alam, M. R.; Mills, K.; Maier, M. A.; Charisse, K.; Sekine, M.; Manoharan, M.; Rajeev, K. G. *J. Org. Chem.* **2011**, *76*, 1198.
(30) Cutler, J. I.; Zheng, D.; Xu, X.; Giljohann, D. A.; Mirkin, C. A. *Nano Lett.* **2010**, *10*, 1477.
(31) Gierlich, J.; Burley, G. A.; Gramlich, P. M. E.; Hammond, D. M.; Carell, T. *Org. Lett.* **2006**, *8*, 3639.
(32) Seela, F.; Sirivolu, V. R. *Chem. Biodiversity* **2006**, *3*, 509.
(33) Berndl, S.; Herzig, N.; Kele, P. t.; Lachmann, D.; Li, X.; Wolfbeis, O. S.; Wagenknecht, H.-A. *Bioconjugate Chem.* **2009**, *20*, 558.
(34) Lietard, J.; Meyer, A.; Vasseur, J.-J.; Morvan, F. *J. Org. Chem.* **2007**, *73*, 191.
(35) Ligeour, C.; Meyer, A.; Vasseur, J.-J.; Morvan, F. *Eur. J. Org. Chem.* **2012**, 1851.
(36) Tanabe, K.; Ando, Y.; Nishimoto, S. *Tetrahedron Lett.* **2011**, *52*, 7135.
(37) Horne, W. S.; Yadav, M. K.; Stout, C. D.; Ghadiri, M. R. *J. Am. Chem. Soc.* **2004**, *126*, 15366.
(38) Dalvie, D. K.; Kalgutkar, A. S.; Khojasteh-Bakht, S. C.; Obach, R. S.; O'Donnell, J. P. *Chem. Res. Toxicol.* **2002**, *15*, 269.
(39) Presumably, a stepwise use of the CuAAC method is also possible which would introduce more than one substituted trizolyl moiety into an ODN.
(40) It is noteworthy that a synthetic route involving bis(*N*,*N*-diisopropylamino)chlorophosphine and sodium acetylide generated the ethynylphosphinyldiamidite which was used as a precursor for synthesizing mono and bicyclic phosphorus heterocycles. See: Timmer, M. S. M.; Ovaa, H.; Filippov, D. V.; van der Marel, G. A.; van Boom, J. H. *Tetrahedron Lett.* **2001**, *42*, 8231.
(41) Iyer, R. P.; Egan, W.; Regan, J. B.; Beaucage, S. L. *J. Am. Chem. Soc.* **1990**, *112*, 1253.
(42) Oligonucleotides (greater than ∼15 bases) stick to the CPG-solid support when anhydrous toluene−ethylene diamine mixture is used for cleavage;
(43) Liu, X.-M.; Quan, L.-d.; Tian, J.; Laquer, F. C.; Ciborowski, P.; Wang, D. *Biomacromolecules* **2010**, *11*, 2621.
(44) Kanan, M. W.; Rozenman, M. M.; Sakurai, K.; Snyder, T. M.; Liu, D. R. *Nature* **2004**, *431*, 545.
(45) Chen, Z.; Meng, H.; Xing, G.; Chen, C.; Zhao, Y.; Jia, G.; Wang, T.; Yuan, H.; Ye, C.; Zhao, F.; Chai, Z.; Zhu, C.; Fang, X.; Ma, B.; Wan, L. *Toxicol. Lett.* **2006**, *163*, 109.
(46) Hein, C.; Liu, X.-M.; Wang, D. *Pharm. Res.* **2008**, *25*, 2216.
(47) Izatt, R. M.; Christensen, J. J.; Rytting, J. H. *Chem. Rev.* **1971**, *71*, 439.
(48) Eichhorn, G. L.; Shin, Y. A. *J. Am. Chem. Soc.* **1968**, *90*, 7323.
(49) Eichhorn, G. L.; Clark, P. *Proc. Natl. Acad. Sci. U.S.A.* **1965**, *53*, 586.
(50) Bach, D.; Miller, I. R. *Biopolymers* **1967**, *5*, 161.
(51) Sagripanti, J.-L.; Goering, P. L.; Lamanna, A. *Toxicol. Appl. Pharmacol.* **1991**, *110*, 477.
(52) Anisimova, N. A.; Kuzhaeva, A. A.; Berkova, G. A.; Deiko, L. I.; Berestovitskaya, V. M. *Russ. J. Gen. Chem.* **2005**, *75*, 689.
(53) Mukai, S.; Flematti, G.; Byrne, L.; Besant, P.; Attwood, P.; Piggott, M. *Amino Acids* **2011**, DOI: 10.1007/s00726-011-1145-2.
(54) Hausheer, F. H.; Singh, U. C.; Palmer, T. C.; Saxe, J. D. *J. Am. Chem. Soc.* **1990**, *112*, 9468.

(55) Okonogi, T. M.; Alley, S. C.; Harwood, E. A.; Hopkins, P. B.; Robinson, B. H. *Proc. Natl. Acad. Sci. U.S.A.* **2002**, *99*, 4156.
(56) Manoharan, M. *Antisense Nucleic Acid Drug Dev.* **2002**, *12*, 103.
(57) Levis, J. T.; Butler, W. O.; Tseng, B. Y.; Ts'O, P. O. P. *Antisense Res. Dev.* **1995**, *5*, 251.
(58) Quartin, R. S.; Brakel, C. L.; Wetmur, G. *Nucleic Acids Res.* **1989**, *17*, 7253.
(59) Dash, C.; Scarth, B. J.; Badorrek, C.; Götte, M.; Le Grice, S. F. J. *Nucleic Acids Res.* **2008**, *36*, 6363.
(60) Dias, N.; Stein, C. A. *Mol. Cancer Ther.* **2002**, *1*, 347.
(61) Miller, P. S.; McParland, K. B.; Jayaraman, K.; Tso, P. O. P. *Biochemistry* **1981**, *20*, 1874.
(62) Thatcher, G. R. J.; Campbell, A. S. *J. Org. Chem.* **1993**, *58*, 2272.
(63) Monia, B. P.; Sasmor, H.; Johnston, J. F.; Freier, S. M.; Lesnik, E. A.; Muller, M.; Geiger, T.; Altmann, K.-H.; Moser, H.; Fabbro, D. *Proc. Natl. Acad. Sci. U.S.A.* **1996**, *93*, 15481.
(64) Kočalka, P.; Andersen, N. K.; Jensen, F.; Nielsen, P. *ChemBioChem* **2007**, *8*, 2106.
(65) Freier, S. M.; Altmann, K.-H. *Nucleic Acids Res.* **1997**, *25*, 4429.
(66) Kibler-Herzog, L.; Zon, G.; Uznanski, B.; Whittier, G.; Wilson, W. D. *Nucleic Acids Res.* **1991**, *19*, 2979.
(67) Kaur, H.; Wengel, J.; Maiti, S. *Biochem. Biophys. Res. Commun.* **2007**, *352*, 118.
(68) Géci, I.; Filichev, V. V.; Pedersen, E. B. *Chem.—Eur. J.* **2007**, *13*, 6379.
(69) Maag, D.; Castro, C.; Hong, Z.; Cameron, C. E. *J. Biol. Chem.* **2001**, *276*, 46094.
(70) Meldal, M.; Tornøe, C. W. *Chem. Rev.* **2008**, *108*, 2952.
(71) Nnane, I. P.; Njar, V. C. O.; Brodie, A. A. *J. Steroid Biochem. Mol. Biol.* **2001**, *78*, 241.
(72) Liu, X.; Wu, J.; Yammine, M.; Zhou, J.; Posocco, P.; Viel, S.; Liu, C.; Ziarelli, F.; Fermeglia, M.; Pricl, S.; Victorero, G.; Nguyen, C.; Erbacher, P.; Behr, J.-P.; Peng, L. *Bioconjugate Chem.* **2011**, *22*, 2461.
(73) Gagnon, K. T.; Watts, J. K.; Pendergraff, H. M.; Montaillier, C.; Thai, D.; Potier, P.; Corey, D. R. *J. Am. Chem. Soc.* **2011**, *133*, 8404.
(74) Francavilla, C.; Low, E.; Nair, S.; Kim, B.; Shiau, T. P.; Debabov, D.; Celeri, C.; Alvarez, N.; Houchin, A.; Xu, P.; Najafi, R.; Jain, R. *Bioorg. Med. Chem. Lett.* **2009**, *19*, 2731.
(75) Gao, Y.; Zhang, Z.; Chen, L.; Gu, W.; Li, Y. *Biomacromolecules* **2009**, *10*, 2175.
(76) Shoji, Y.; Akhtar, S.; Periasamy, A.; Herman, B.; Juliano, R. L. *Nucleic Acids Res.* **1991**, *19*, 5543.
(77) Shoji, Y.; Shimada, J.; Mizushima, Y.; Iwasawa, A.; Nakamura, Y.; Inouye, K.; Azuma, T.; Sakurai, M.; Nishimura, T. *Antimicrob. Agents Chemother.* **1996**, *40*, 1670.
(78) Jordan, E. T.; Collins, M.; Terefe, J.; Ugozzoli, L.; Rubio, T. *J. Biomol. Tech.* **2008**, *19*, 328.
(79) Morvan, F.; Castex, C.; Vivès, E.; Imbach, J.-L. *Nucleosides, Nucleotides Nucleic Acids* **2001**, *20*, 805.
(80) Pack, D. W.; Putnam, D.; Langer, R. *Biotechnol. Bioeng.* **2000**, *67*, 217.
(81) Juliano, R. L.; Ming, X.; Nakagawa, O. *Bioconjugate Chem.* **2012**, *23*, 147.
(82) Angers, C. G.; Merz, A. J. *Semin. Cell Dev. Biol.* **2011**, *22*, 18.
(83) Li, B.; Hughes, J. A.; Phillips, M. I. *Neurochem. Int.* **1997**, *31*, 393.
(84) Beltinger, C.; Saragovi, H. U.; Smith, R. M.; LeSauteur, L.; Shah, N.; DeDionisio, L.; Christensen, L.; Raible, A.; Jarett, L.; Gewirtz, A. M. *J. Clin. Invest.* **1995**, *95*, 1814.
(85) Wingens, M.; van Hooijdonk, C. A. E. M.; de Jongh, G. J.; Schalkwijk, J.; van Erp, P. E. J. *Arch. Dermatol. Res.* **1998**, *290*, 119.
(86) Singh, R.; Kumar, S.; Nada, R.; Prasad, R. *Mol. Cell. Biochem.* **2006**, *282*, 13.
(87) Aston, N. S.; Watt, N.; Morton, I. E.; Tanner, M. S.; Evans, G. S. *Hum. Exp. Toxicol.* **2000**, *19*, 367.
(88) Hultberg, B.; Andersson, A.; Isaksson, A. *Toxicology* **1997**, *117*, 89.
(89) Gramlich, P. M. E.; Warncke, S.; Gierlich, J.; Carell, T. *Angew. Chem., Int. Ed.* **2008**, *47*, 3442.